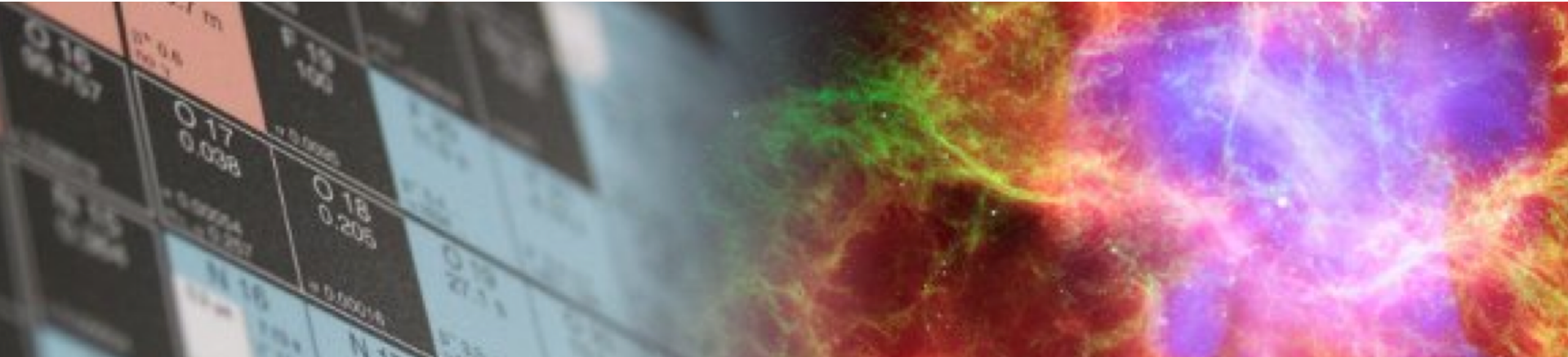


Chiral effective field theory for dark matter direct detection

Achim Schwenk



TECHNISCHE
UNIVERSITÄT
DARMSTADT



SFB 1044 Workshop, Mainz, Oct. 1, 2018

DFG



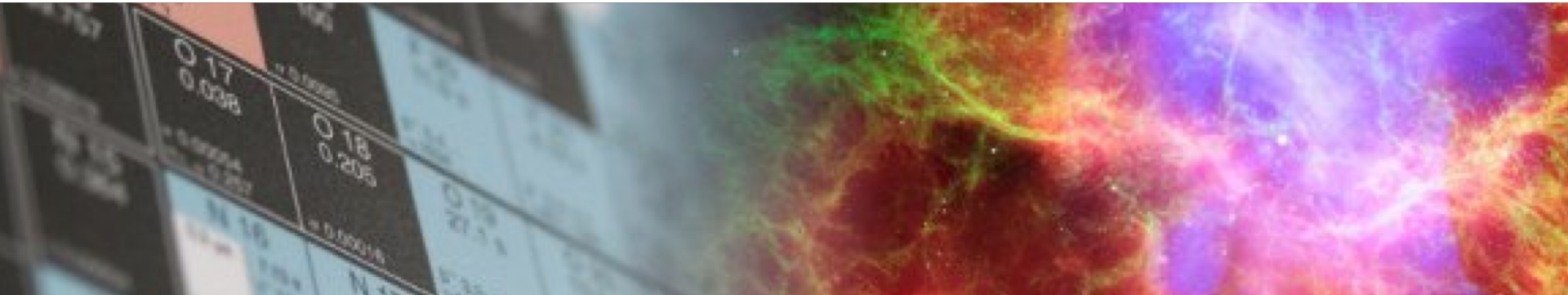
Bundesministerium
für Bildung
und Forschung



Chiral EFT for dark matter direct detection

Speakers

 Achim DENIG



SFB 1044 Workshop, Mainz, Oct. 1, 2018

DFG



Bundesministerium
für Bildung
und Forschung

 **HELMHOLTZ**
ASSOCIATION

DM in direct detection

Assume DM particle is WIMP, search strategies:

Direct detection:

WIMP scattering off nuclei, needs as input

Nucleon matrix elements

WIMP-quark/gluon couplings in nucleons

Nuclear structure factors

sensitive to nuclear physics

relevant momentum transfers $\sim m_\pi$

calculate systematically with chiral EFT

Menéndez et al., PRD (2012), Klos et al., PRD (2013),

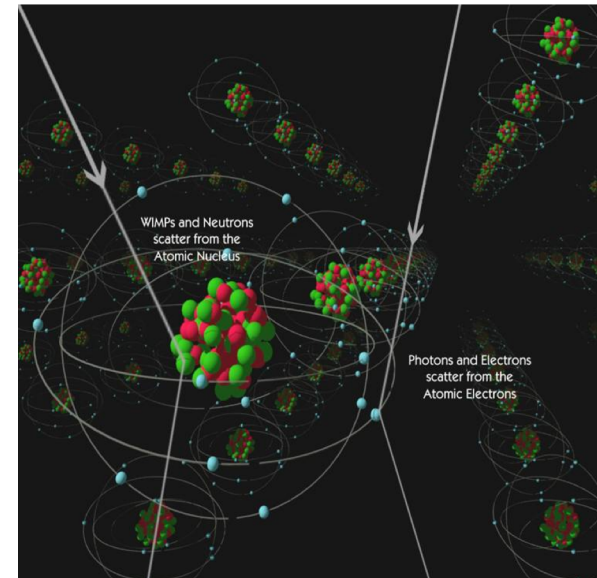
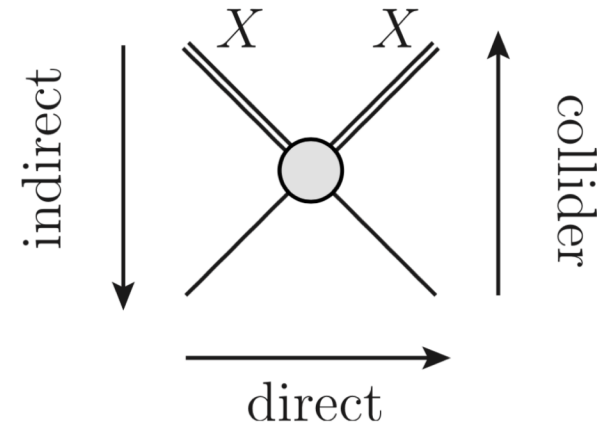
Baudis et al., PRD (2013), Vietze et al., PRD (2015),

Hoferichter et al., PLB (2015), Hoferichter et al., PRD (2016)

Hoferichter et al., PRL (2017), Fieguth et al., PRD (2018)

incorporate what we know about **QCD/nuclear physics**

see also Prézeau et al., PRL (2003), Cirigliano et al., JHEP (2012), PLB (2014), Hill and Solon, PRD (2015), Körber et al., PRC (2017), Bishara et al., JCAP (2017), Gadza et al., PRC (2017)



Scales in DM direct detection

BSM scale: WIMPs coupling to q, g via exchange particles

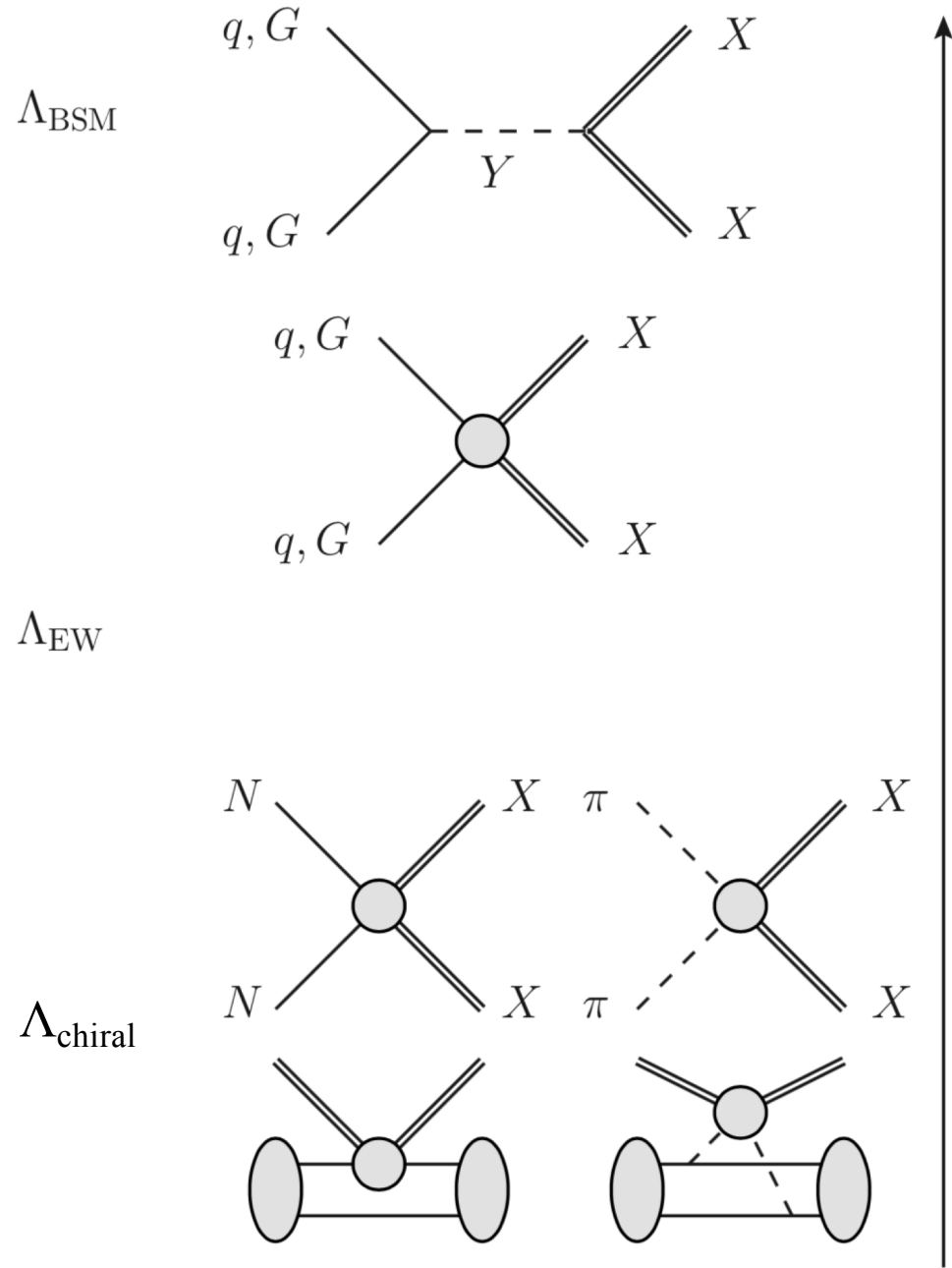
SM + **effective operators**

$$\mathcal{L}_{\text{SM}} + \sum_{i,k} \frac{1}{\Lambda_{\text{BSM}}^i} \mathcal{O}_{i,k}$$

Integrate out **EW physics**

Chiral EFT scale: WIMP coupling to nucleons and pions

Nuclear structure: embedding chiral EFT operators in nucleus



Chiral EFT for nuclear forces

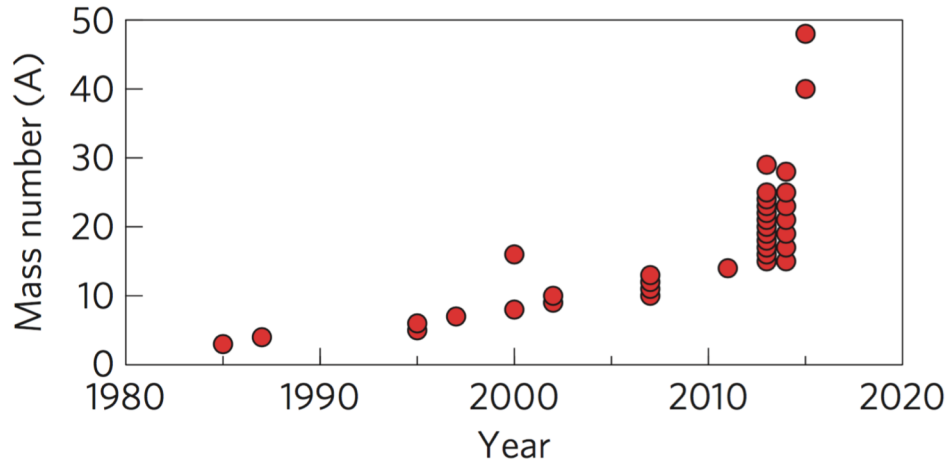
Separation of scales: low momenta $\frac{1}{\lambda} = Q \ll \Lambda_b$ breakdown scale ~ 500 MeV

	NN	3N	4N	
LO $\mathcal{O}\left(\frac{Q^0}{\Lambda^0}\right)$				include long-range pion physics
NLO $\mathcal{O}\left(\frac{Q^2}{\Lambda^2}\right)$				few short-range couplings, fit to experiment once
N ² LO $\mathcal{O}\left(\frac{Q^3}{\Lambda^3}\right)$				consistent electroweak interactions and matching to lattice QCD
N ³ LO $\mathcal{O}\left(\frac{Q^4}{\Lambda^4}\right)$				from quarks to nucleons/pions for coupling to beyond SM particles
	+ ...	(2011) ...	(2006) ...	

Weinberg, van Kolck, Kaplan, Savage, Wise, Bernard, Epelbaum, Kaiser, Machleidt, Meissner,...

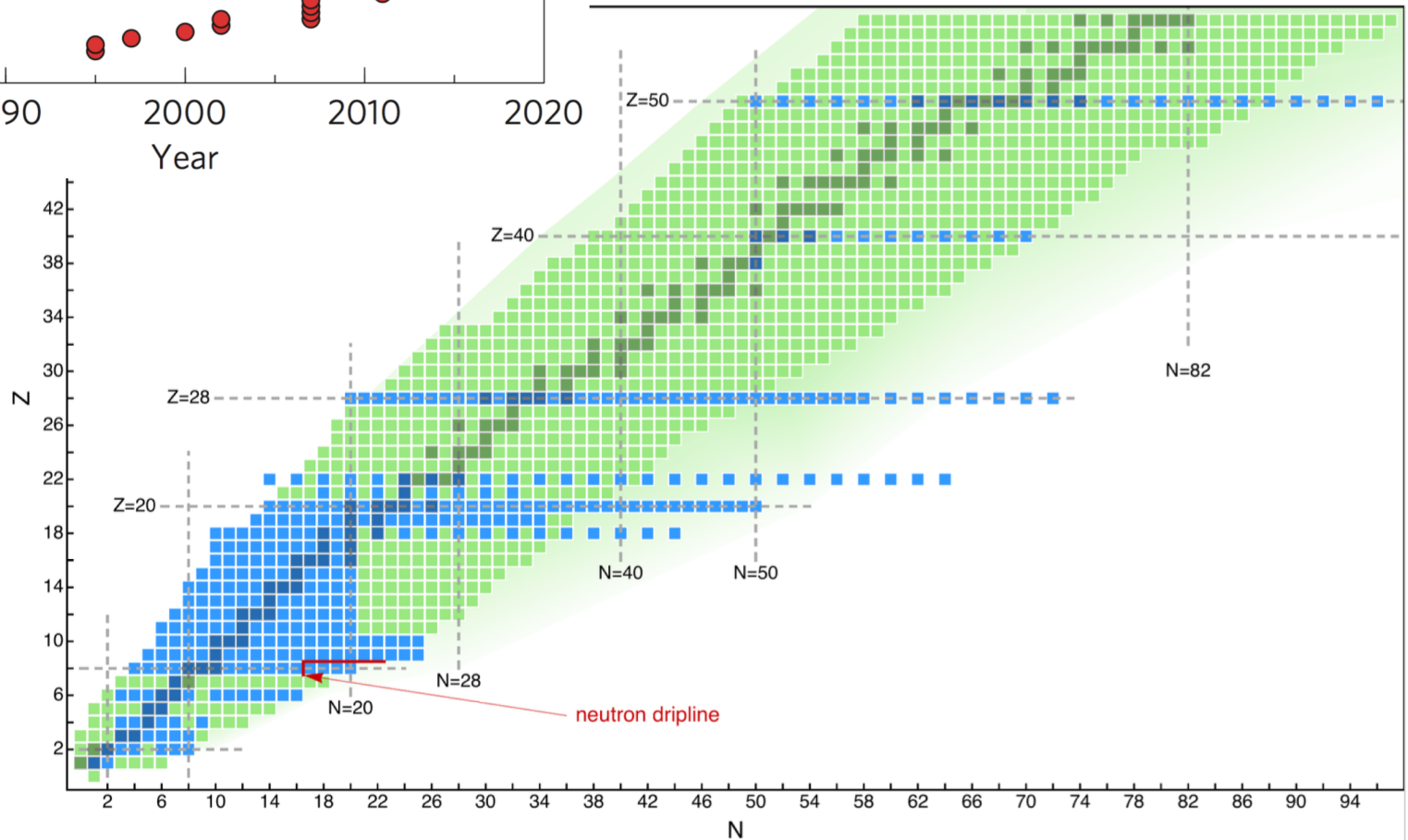
Progress in ab initio calculations of nuclei

dramatic progress in last 5 years to access nuclei up to $A \sim 50$



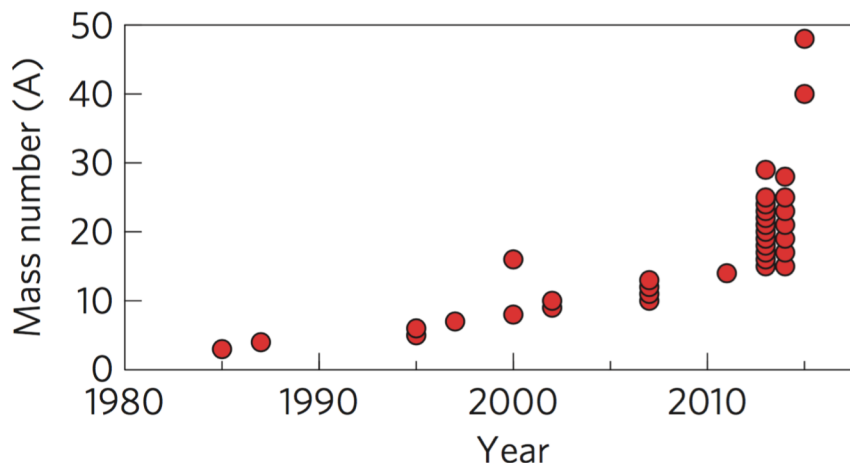
from Hagen et al., Nature Phys. (2016)

from Hergert et al., Phys. Rep. (2016)



Progress in ab initio calculations of nuclei

dramatic progress in last 5 years to access nuclei up to $A \sim 50$



LETTER

doi:10.1038/nature12226

Masses of exotic calcium isotopes pin down nuclear forces

F. Wienholtz¹, D. Beck², K. Blaum³, Ch. Borgmann³, M. Breitenfeldt⁴, R. B. Cakirli^{3,5}, S. George¹, F. Herfurth², J. D. Holt^{6,7}, M. Kowalska⁸, S. Kreim^{3,8}, D. Lunney⁹, V. Manea⁹, J. Menéndez^{6,7}, D. Neidherr², M. Rosenbusch¹, L. Schweikhard¹, A. Schwenk^{7,6}, J. Simonis^{6,7}, J. Stania¹⁰, R. N. Wolf¹ & K. Zuber¹⁰

doi:10.1038/nature12522

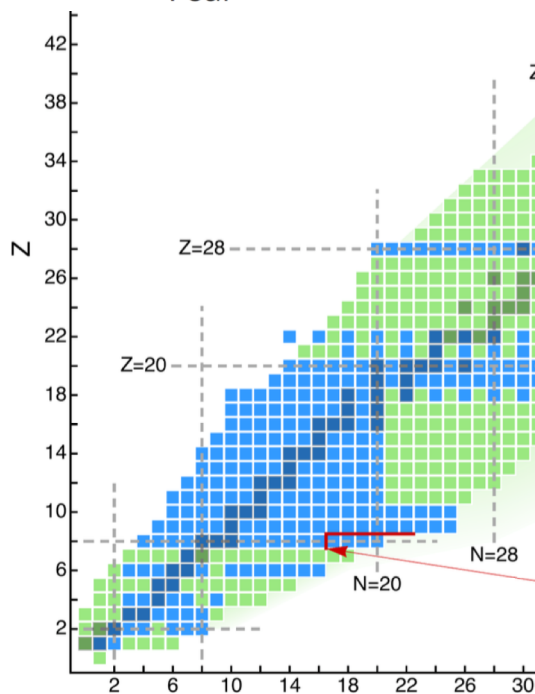
Evidence for a new nuclear ‘magic number’ from the level structure of ⁵⁴Ca

D. Steppenbeck¹, S. Takeuchi², N. Aoi³, P. Doornenbal², M. Matsushita¹, H. Wang², H. Baba², N. Fukuda², S. Go¹, M. Honma⁴, J. Lee², K. Matsui⁵, S. Michimasa¹, T. Motobayashi², D. Nishimura⁶, T. Otsuka^{1,5}, H. Sakurai^{2,5}, Y. Shiga⁷, P.-A. Söderström², T. Sumikama⁸, H. Suzuki², R. Taniuchi⁵, Y. Utsuno⁹, J. J. Valiente-Dobón¹⁰ & K. Yoneda²

ARTICLES

PUBLISHED ONLINE: 2 NOVEMBER 2015 | DOI: 10.1038/NPHYS3529

nature
physics



Neutron and weak-charge distributions of the ⁴⁸Ca nucleus

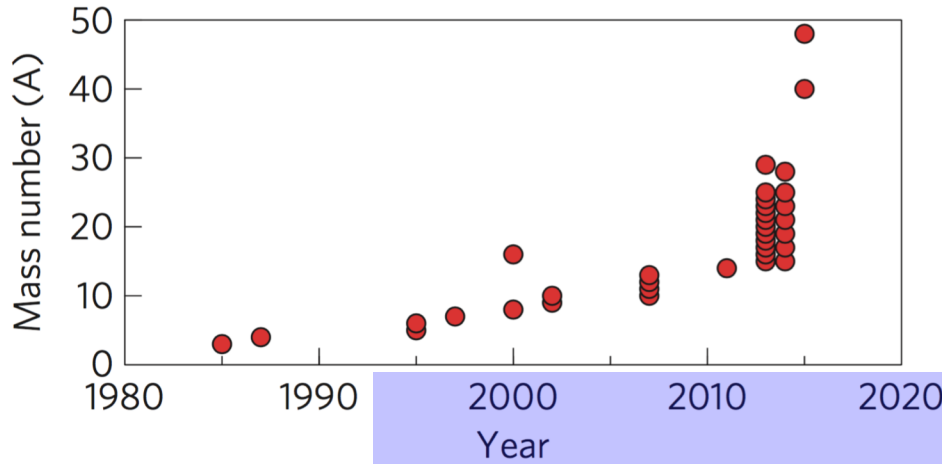
G. Hagen^{1,2*}, A. Ekström^{1,2}, C. Forssén^{1,2,3}, G. R. Jansen^{1,2}, W. Nazarewicz^{1,4,5}, T. Papenbrock^{1,2}, K. A. Wendt^{1,2}, S. Bacca^{6,7}, N. Barnea⁸, B. Carlsson³, C. Drischler^{9,10}, K. Hebeler^{9,10}, M. Hjorth-Jensen^{4,11}, M. Miorelli^{6,12}, G. Orlandini^{13,14}, A. Schwenk^{9,10} and J. Simonis^{9,10}

Unexpectedly large charge radii of neutron-rich calcium isotopes

R. F. Garcia Ruiz^{1*}, M. L. Bissell^{1,2}, K. Blaum³, A. Ekström^{4,5}, N. Frömmgen⁶, G. Hagen⁴, M. Hammen⁶, K. Hebeler^{7,8}, J. D. Holt⁹, G. R. Jansen^{4,5}, M. Kowalska¹⁰, S. Kreim³, W. Nazarewicz^{4,11,12}, R. Neugart^{3,6}, G. Neyens¹, W. Nörtershäuser^{6,7}, T. Papenbrock^{4,5}, J. Papuga¹, A. Schwenk^{3,7,8}, J. Simonis^{7,8}, K. A. Wendt^{4,5} and D. T. Yordanov^{3,13}

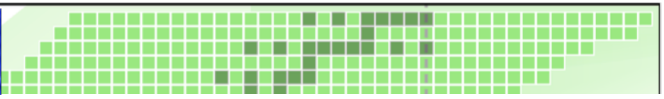
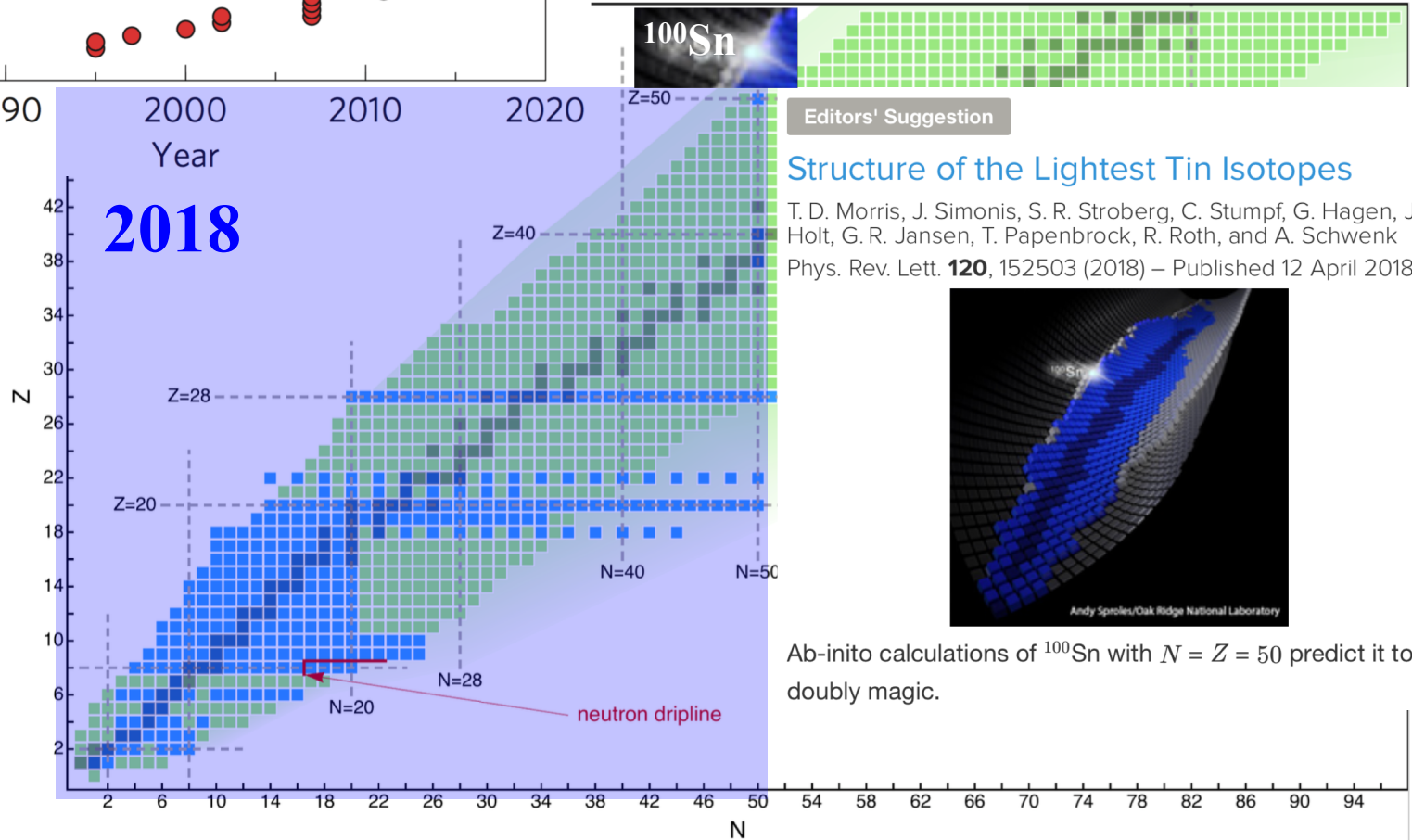
Progress in ab initio calculations of nuclei

dramatic progress in last 5 years to access nuclei up to $A \sim 50$



from Hagen et al., *Nature Phys.* (2016)

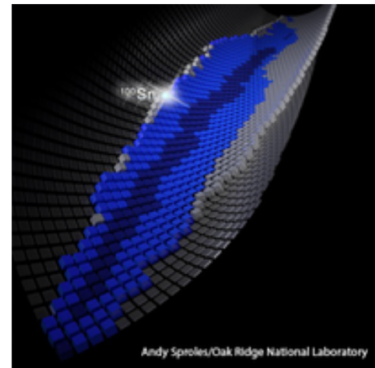
from Hergert et al., *Phys. Rep.* (2016)



Editors' Suggestion

Structure of the Lightest Tin Isotopes

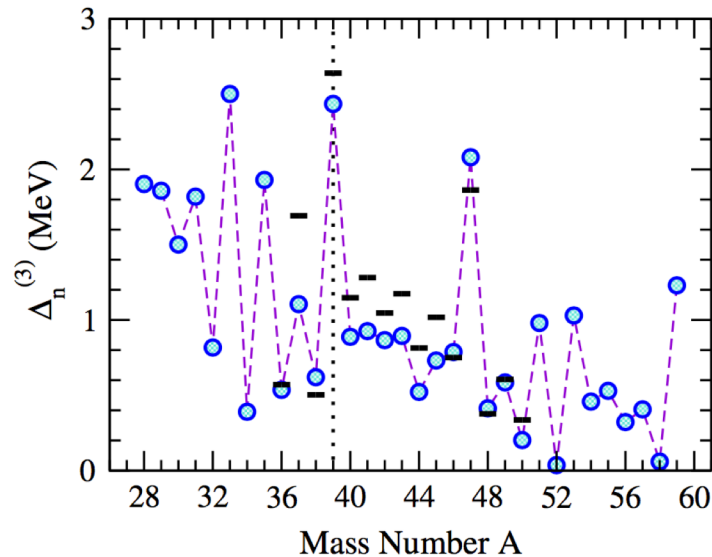
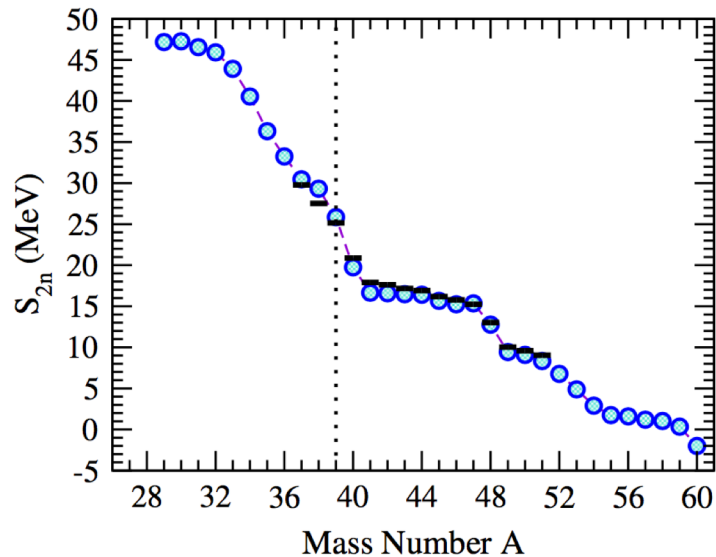
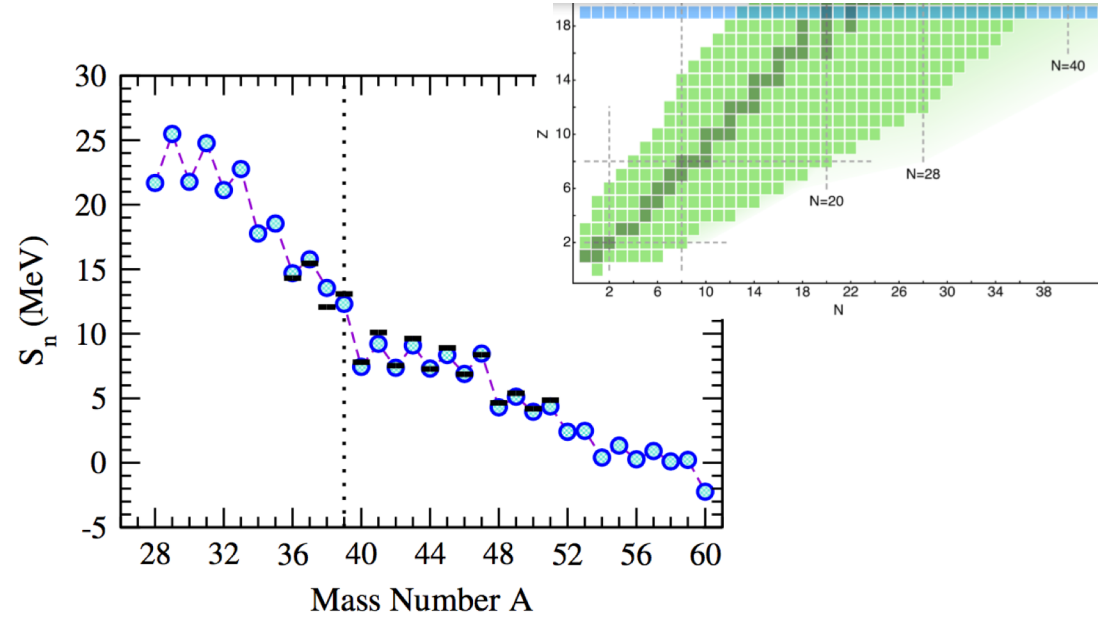
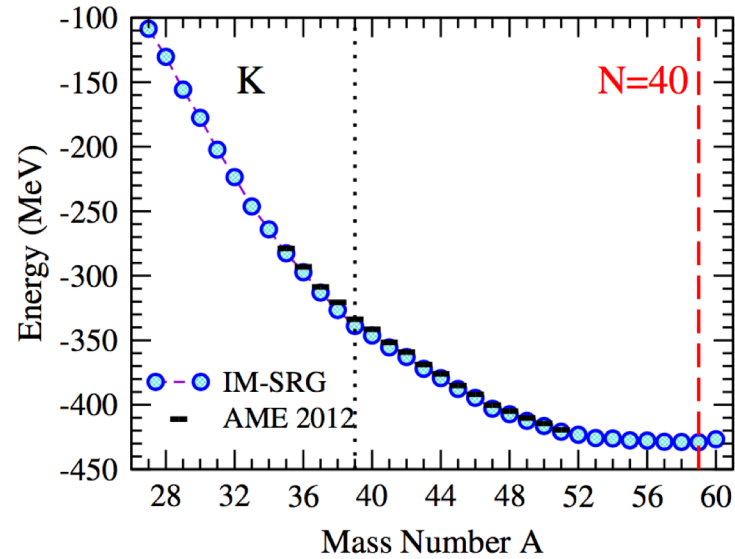
T. D. Morris, J. Simonis, S. R. Stroberg, C. Stumpf, G. Hagen, J. D. Holt, G. R. Jansen, T. Papenbrock, R. Roth, and A. Schwenk
Phys. Rev. Lett. **120**, 152503 (2018) – Published 12 April 2018



Ab-initio calculations of ^{100}Sn with $N = Z = 50$ predict it to be doubly magic.

Ab initio IM-SRG prediction of medium-mass nuclei

Simonis, Stroberg et al., PRC (2017)



Preview

structure factors for **spin-dependent** WIMP scattering
with Klos, Menéndez, Gazit, PRD (2012, 2013)

based on **large-scale nuclear structure calculations** and
systematic expansion of **WIMP-nucleon currents in chiral EFT**

signatures of WIMP **inelastic scattering**
with Baudis et al., PRD (2013)

WIMP-nucleon interactions in chiral EFT to N²LO
with Hoferichter, Klos, PLB (2015)

general coherent (SI+) WIMP-nucleus scattering
with Hoferichter, Klos, Menéndez, PRD (2016)

Linking **LHC and direct detection** results in **Higgs Portals**
with Hoferichter, Klos, Menéndez, PRL (2017)

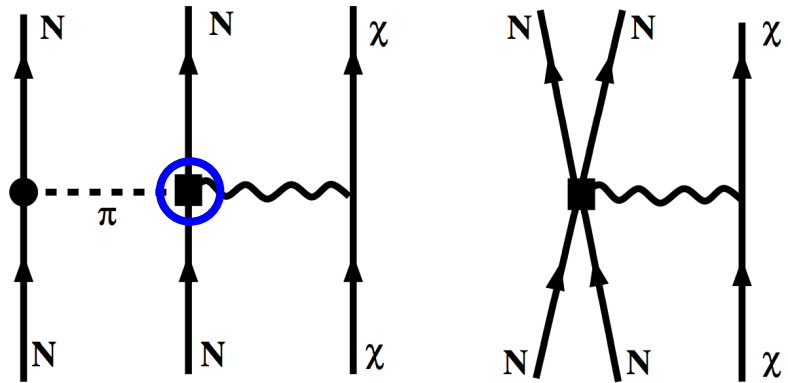
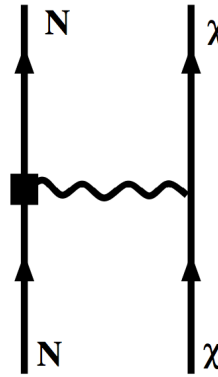
Chiral EFT for coupling to external sources

example: axial-vector currents
one-body currents at Q^0 and Q^2

	NN	3N	4N
LO $\mathcal{O}\left(\frac{Q^0}{\Lambda^0}\right)$			
NLO $\mathcal{O}\left(\frac{Q^2}{\Lambda^2}\right)$			
N ² LO $\mathcal{O}\left(\frac{Q^3}{\Lambda^3}\right)$			
N ³ LO $\mathcal{O}\left(\frac{Q^4}{\Lambda^4}\right)$			
	+ ... (2011) ...	(2011) ...	(2006) ...

derived in (1994/2002)

+ two-body currents at Q^3



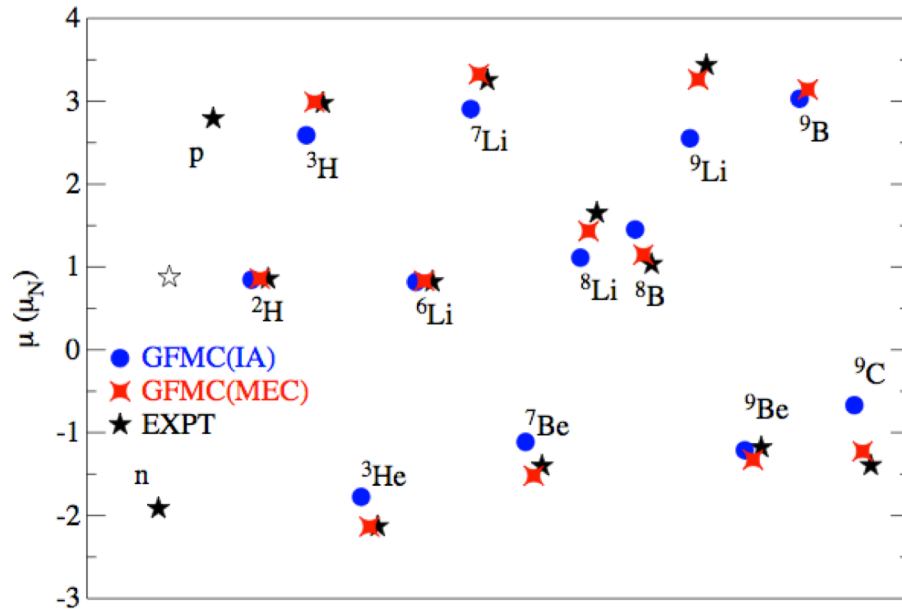
same couplings in forces and currents!

Chiral EFT for electroweak currents

consistent electroweak one- and two-body (meson-exchange) currents

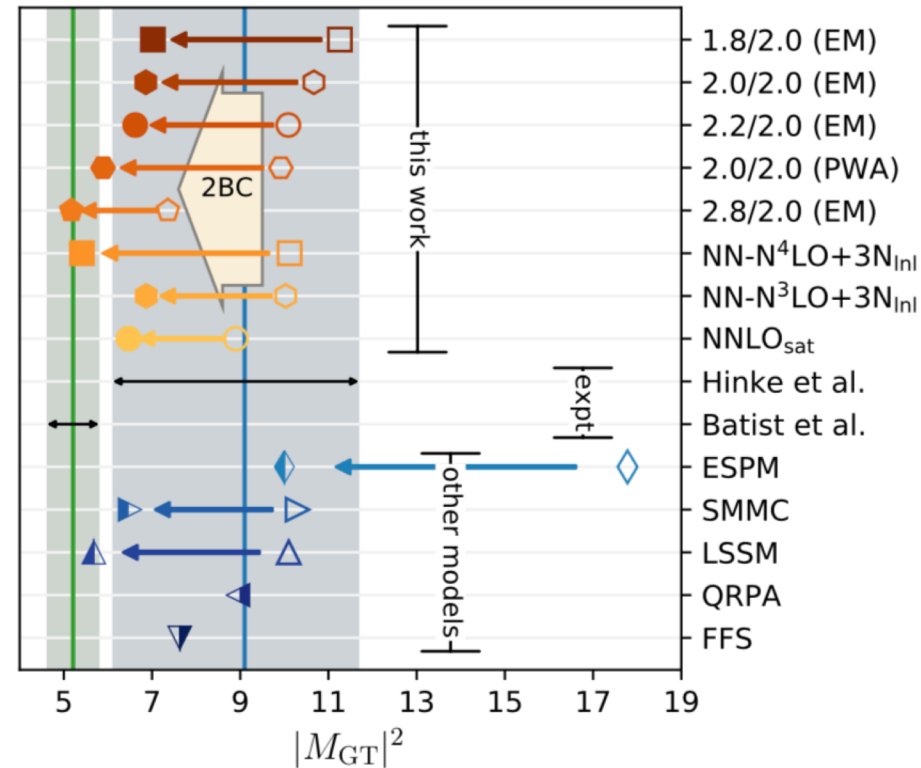
magnetic moments in light nuclei

Pastore et al. (2012-)



Gamow-Teller beta decay of ^{100}Sn

Gysbers, Hagen et al., see Gaute's talk

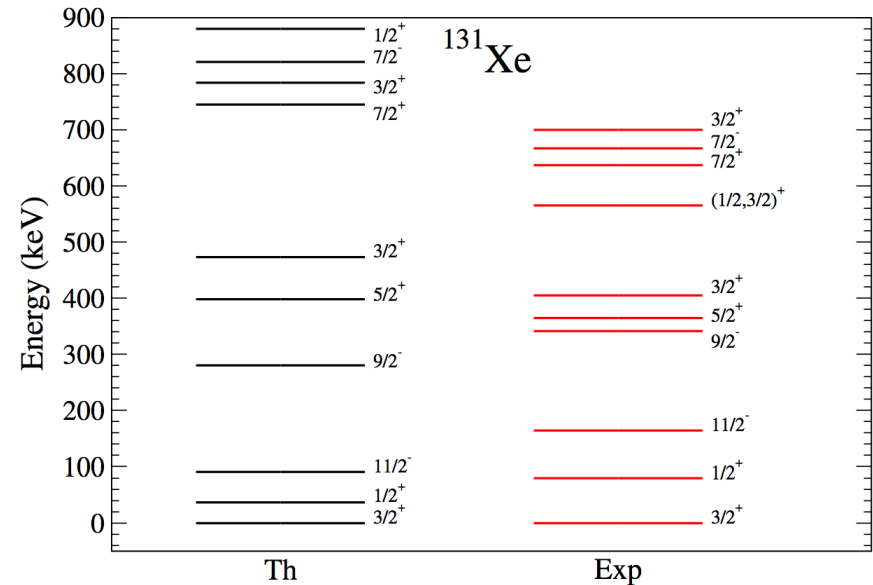
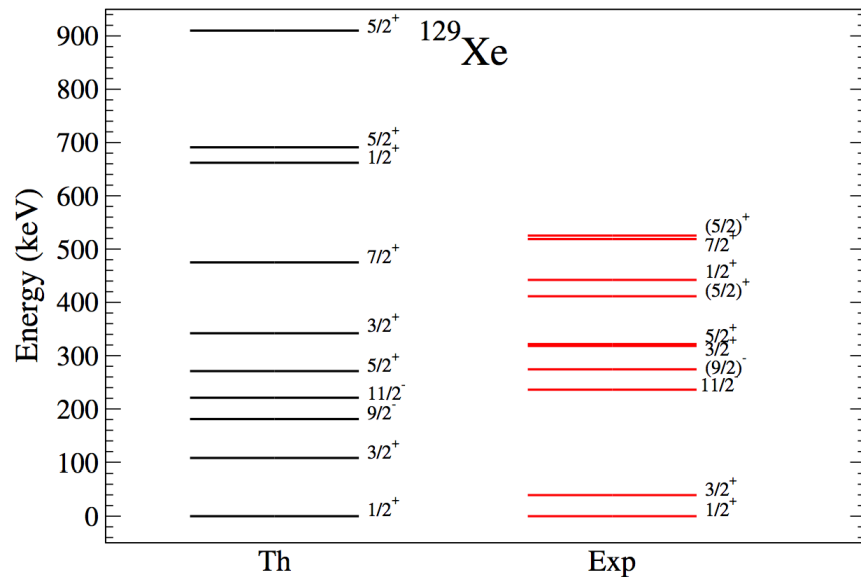


two-body currents are key for quenching puzzle of beta decays

Nuclear structure for direct detection

valence-shell Hamiltonian calculated from NN interactions + corrections to compensate for not including 3N forces (will improve in the future)

valence spaces and interactions have been tested successfully in nuclear structure calculations, largest spaces used



very good agreement for spectra; ordering and grouping well reproduced

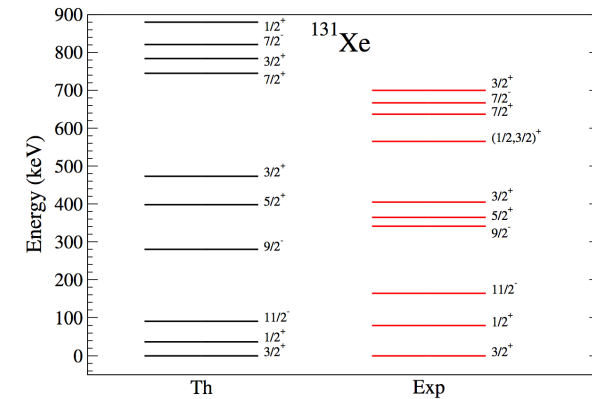
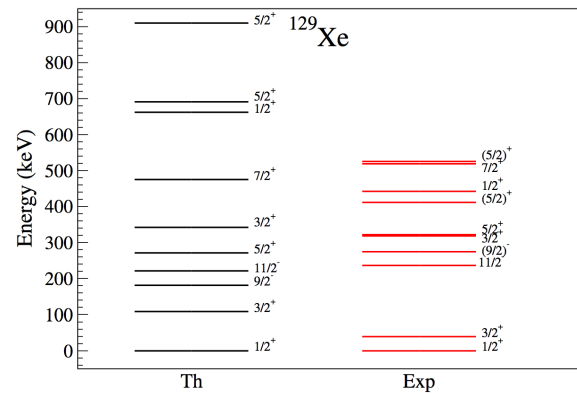
Menendez, Gazit, AS, PRD (2012)

connects WIMP direct detection with double-beta decay

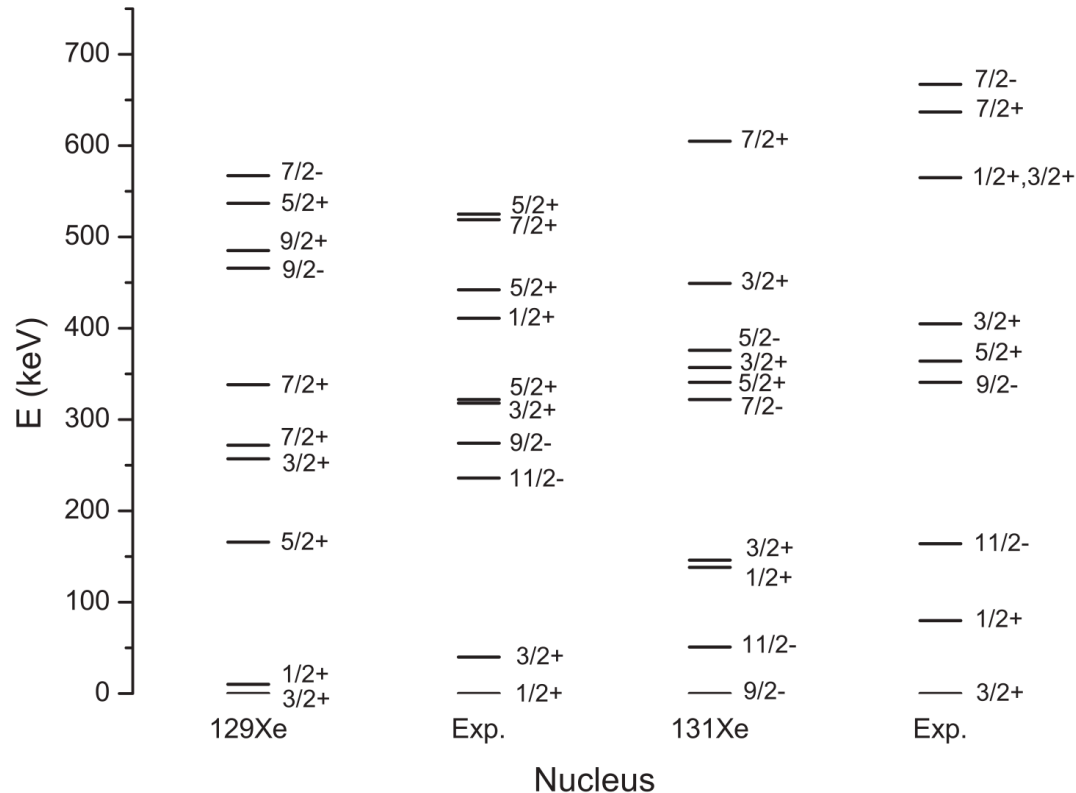
Nuclear structure for direct detection

very good agreement for spectra; ordering and grouping well reproduced

Menendez, Gazit, AS, PRD (2012)



compare to other calculations for WIMP scattering



Nuclear structure factors

differential cross section for spin-dependent WIMP scattering

~ axial-vector structure factor $S_A(p)$ Engel et al. (1992)

$$\begin{aligned}\frac{d\sigma}{dp^2} &= \frac{1}{(2J_i + 1)\pi v^2} \sum_{s_f, s_i} \sum_{M_f, M_i} |\langle f | \mathcal{L}_\chi^{\text{SD}} | i \rangle|^2 \\ &= \frac{8G_F^2}{(2J_i + 1)v^2} S_A(p),\end{aligned}$$

decompose into longitudinal, transverse electric and transverse magnetic

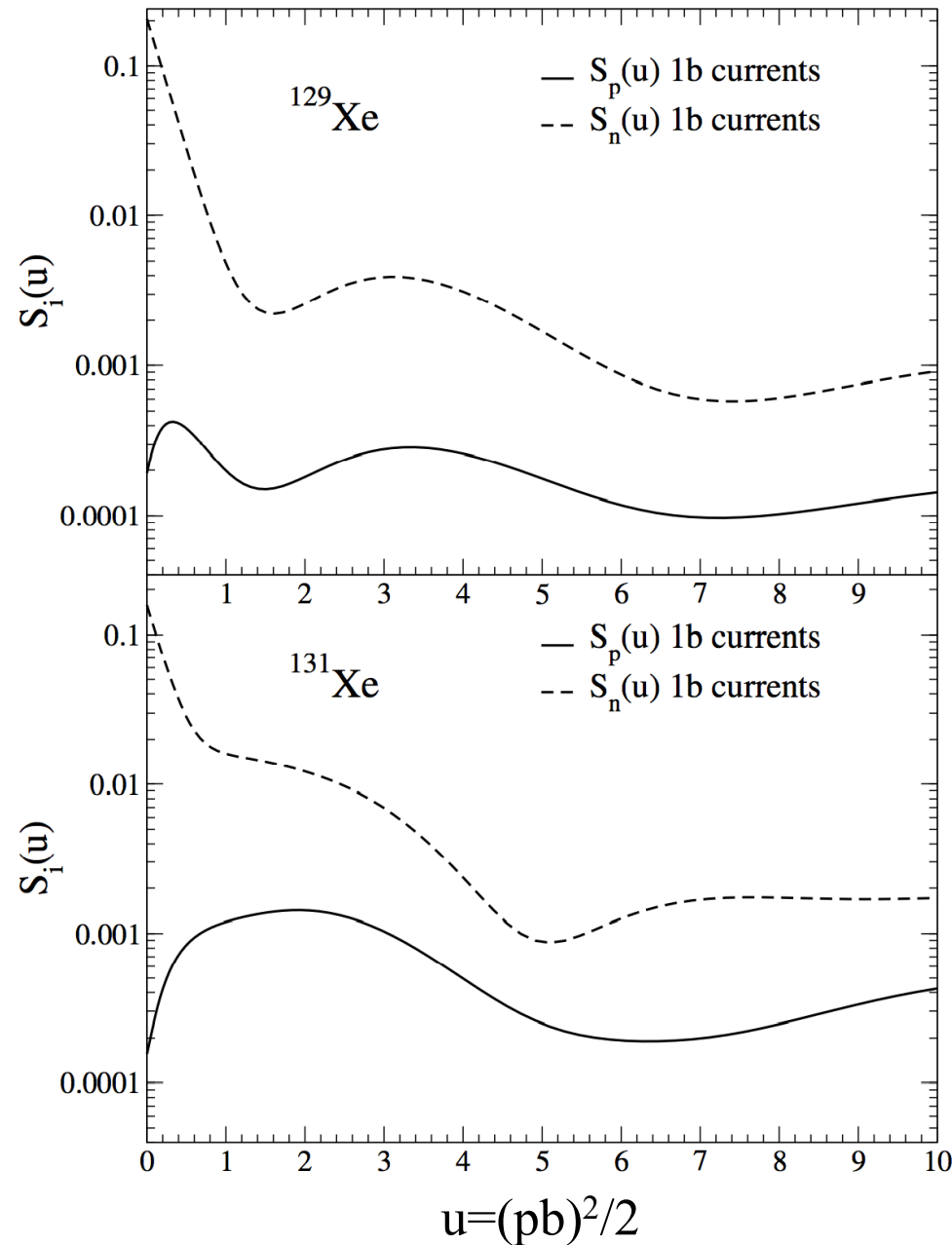
$$\begin{aligned}S_A(p) &= \sum_{L \geq 0} |\langle J_f || \mathcal{L}_L^5 || J_i \rangle|^2 \\ &\quad + \sum_{L \geq 1} \left(|\langle J_f || \mathcal{T}_L^{\text{el}5} || J_i \rangle|^2 + |\langle J_f || \mathcal{T}_L^{\text{mag}5} || J_i \rangle|^2 \right)\end{aligned}$$

transverse magnetic multipoles vanish for elastic scattering

can also decompose into isoscalar/isovector structure factors $S_{ij}(p)$

$$S_A(p) = a_0^2 S_{00}(p) + a_0 a_1 S_{01}(p) + a_1^2 S_{11}(p)$$

Xenon response with one-body currents

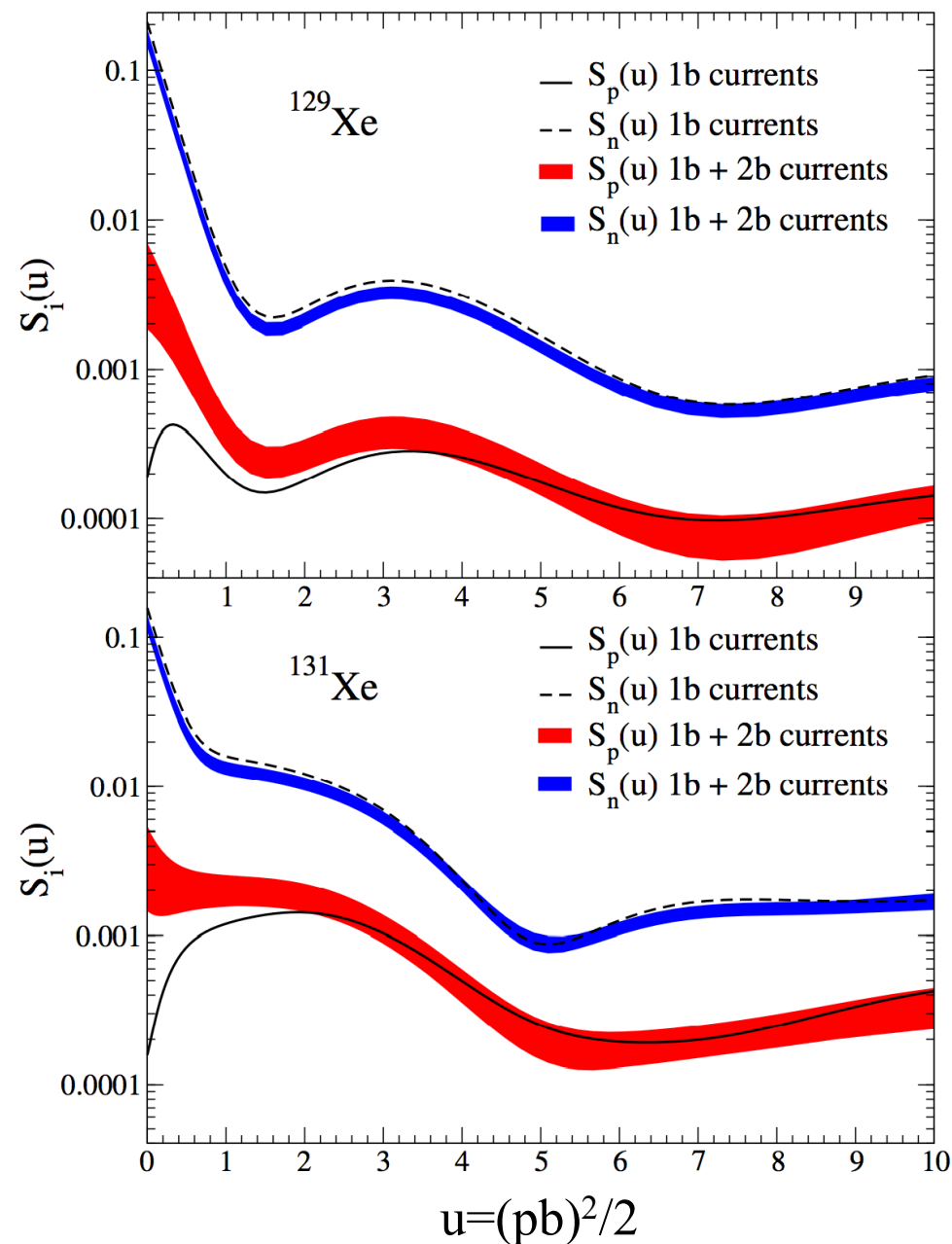


$^{129,131}\text{Xe}$ are even Z , odd N ,
spin is carried mainly by neutrons

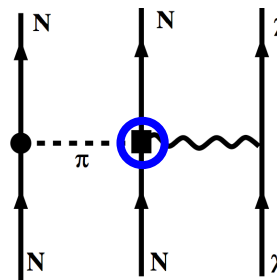
at $p=0$ structure factors
at the level of one-body currents
dominated by “neutron”-only

$$S_A = \frac{(2J+1)(J+1)}{\pi J} |a_p \langle S_p \rangle + a_n \langle S_n \rangle|^2$$

Xenon response with 1+2-body currents



two-body currents due to strong interactions among nucleons

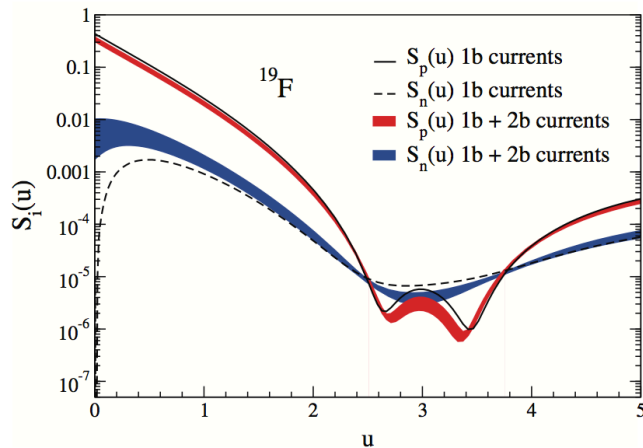


WIMPs couple to neutrons and protons at the same time

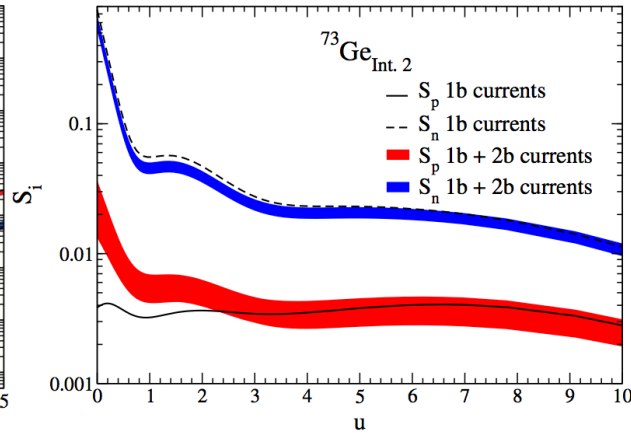
enhances coupling to even species in all cases (protons for Xe)

Spin-dependent WIMP-nucleus response for ^{19}F , ^{23}Na , ^{27}Al , ^{29}Si , ^{73}Ge , ^{127}I

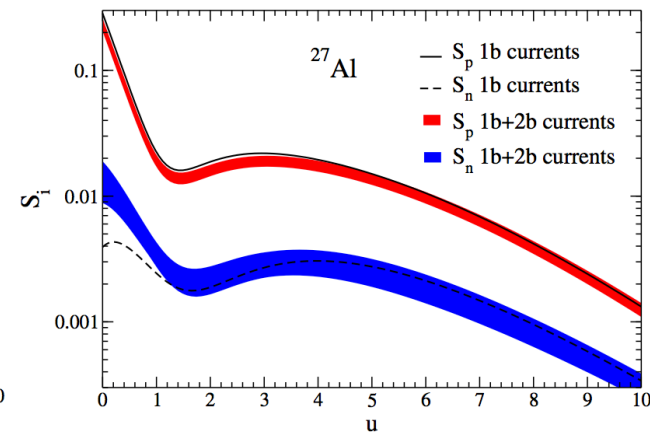
Klos, Menéndez, Gazit, AS, PRD (2013) includes structure factor fits for all isotopes



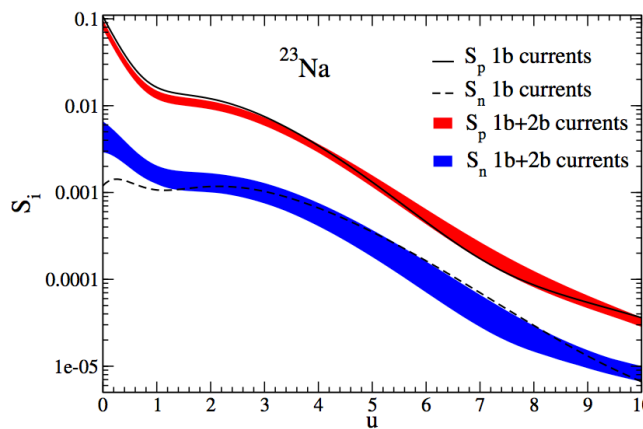
PICASSO, COUPP, SIMPLE



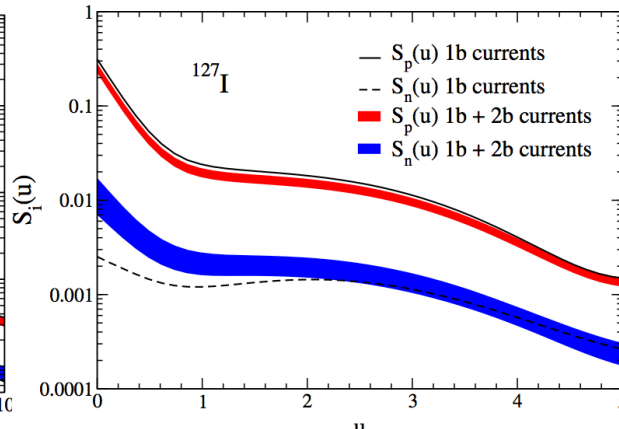
CDMS, EDELWEISS, EURECA



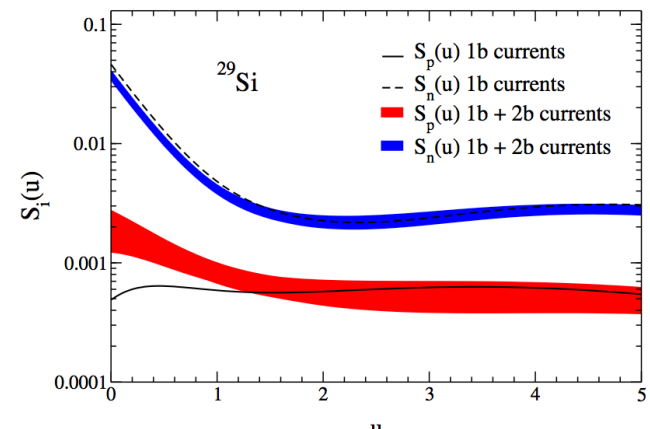
CRESST



DAMA, ANAIS, DM-Ice



DAMA, ANAIS, DM-Ice, KIMS



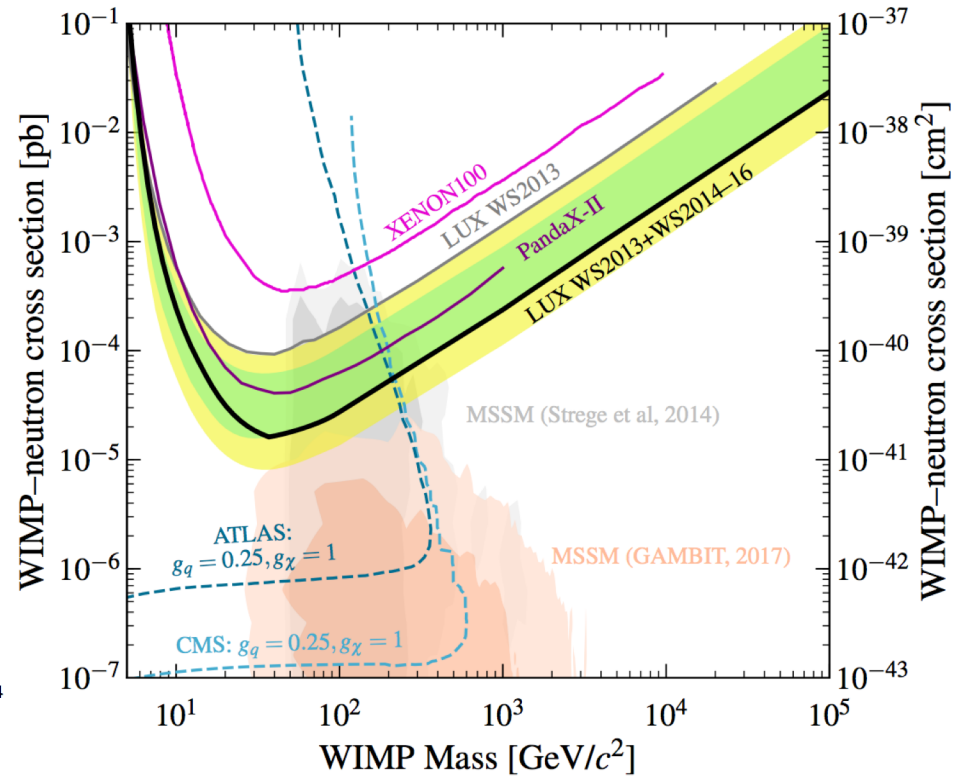
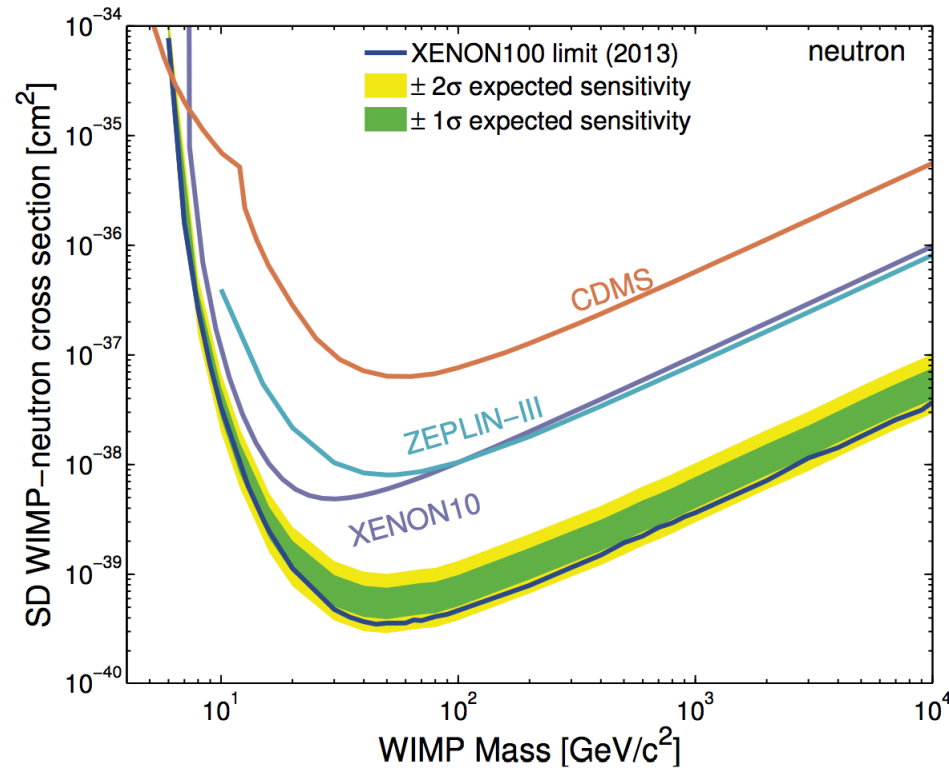
CDMS-II

Limits on SD WIMP-neutron interactions

limits from XENON100 *Aprile et al., PRL (2013)*

PandaX-II *Fu et al., PRL (2017)* and LUX *Akerib et al., PRL (2017)*

used our calculations with uncertainty bands for WIMP currents in nuclei

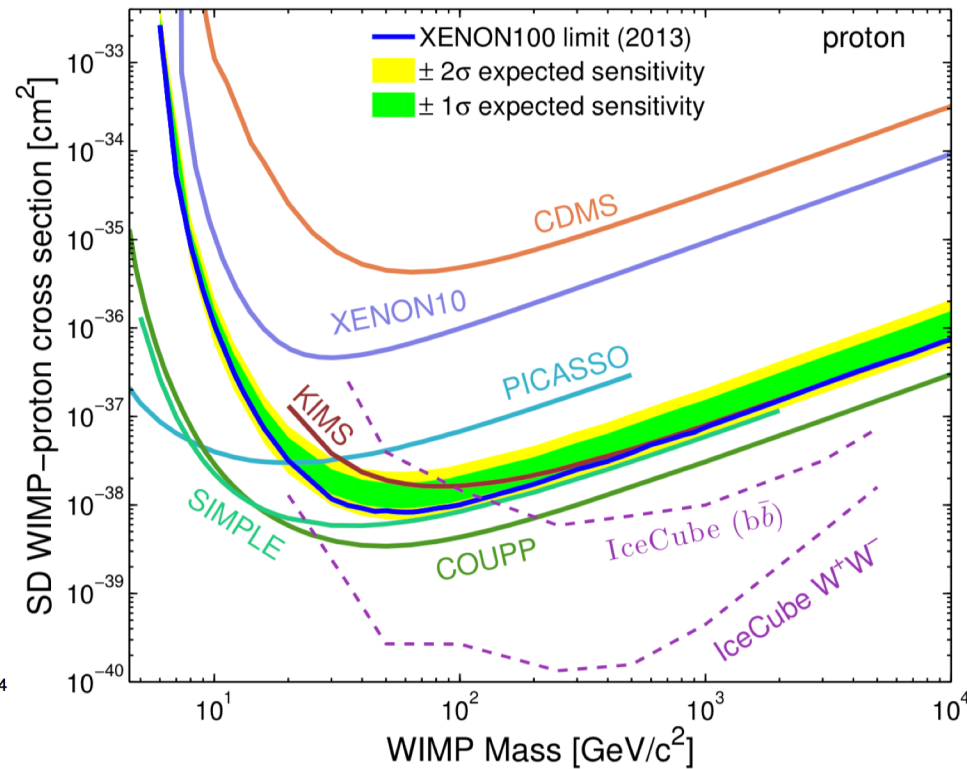
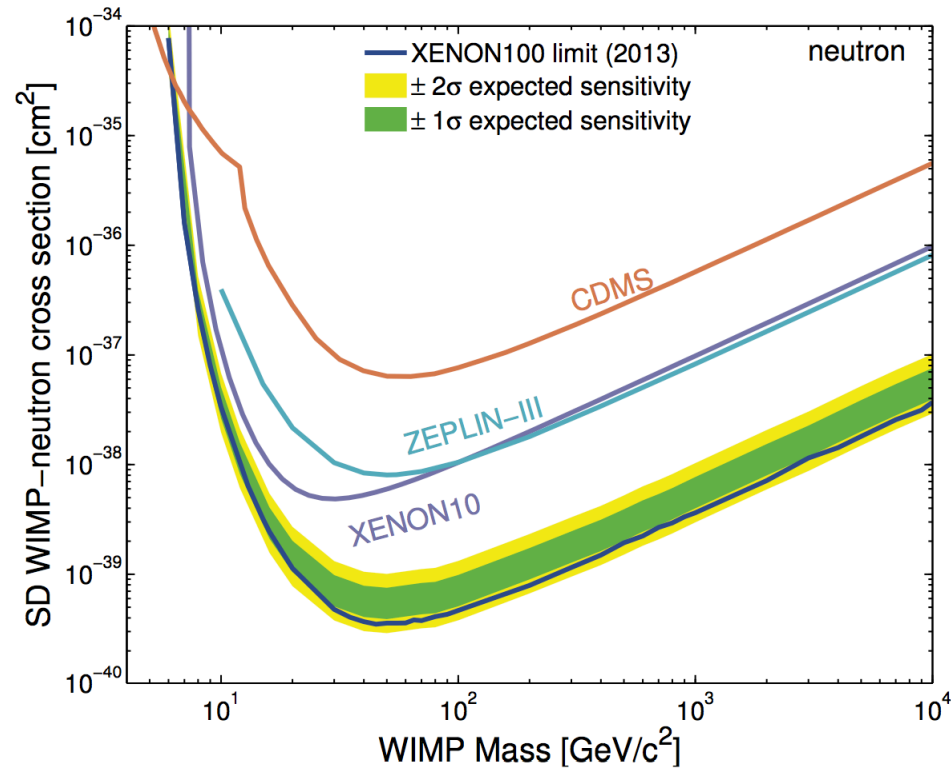


Limits on SD WIMP-proton interactions

limits from XENON100 *Aprile et al., PRL (2013)*

PandaX-II *Fu et al., PRL (2017)* and LUX *Akerib et al., PRL (2017)*

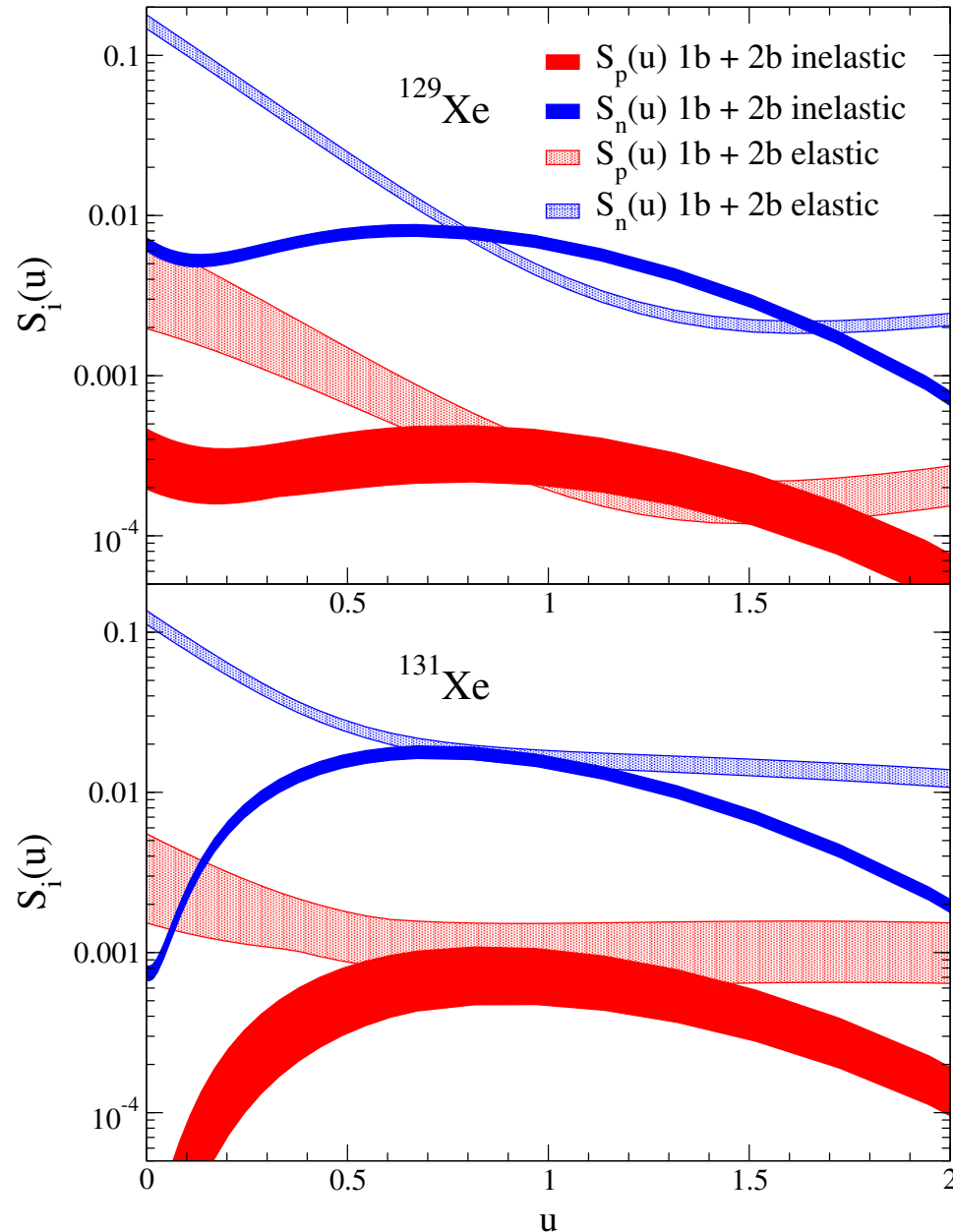
used our calculations with uncertainty bands for WIMP currents in nuclei



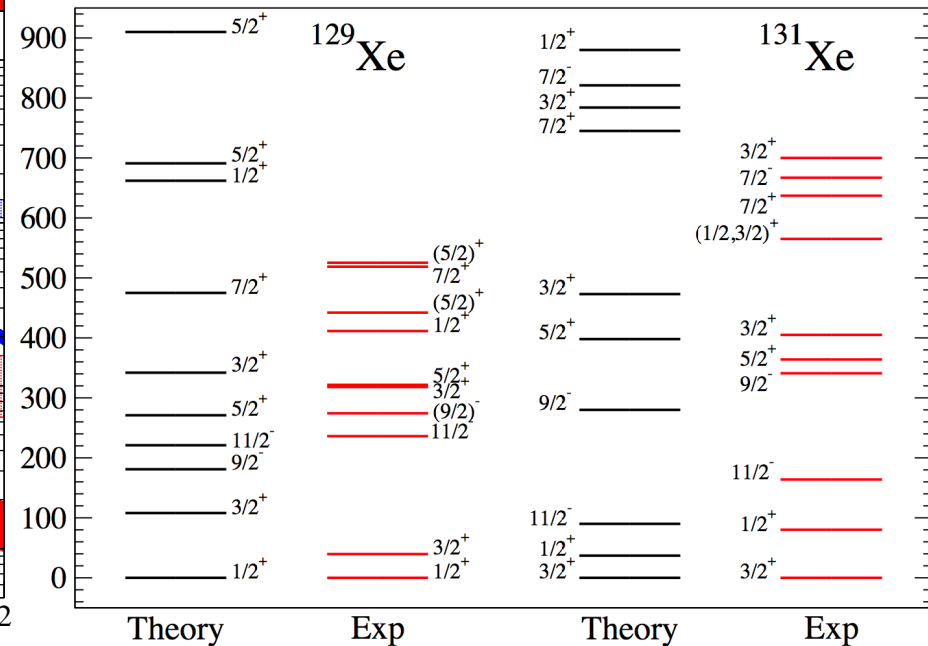
XENON competitive for WIMP-proton coupling due to 2-body currents

Inelastic WIMP scattering to 40 and 80 keV excited states

Baudis, Kessler, Klos, Lang, Menéndez, Reichard, AS, PRD (2013)



inelastic channel
comparable/dominates elastic
channel for
 $p \sim 150$ MeV

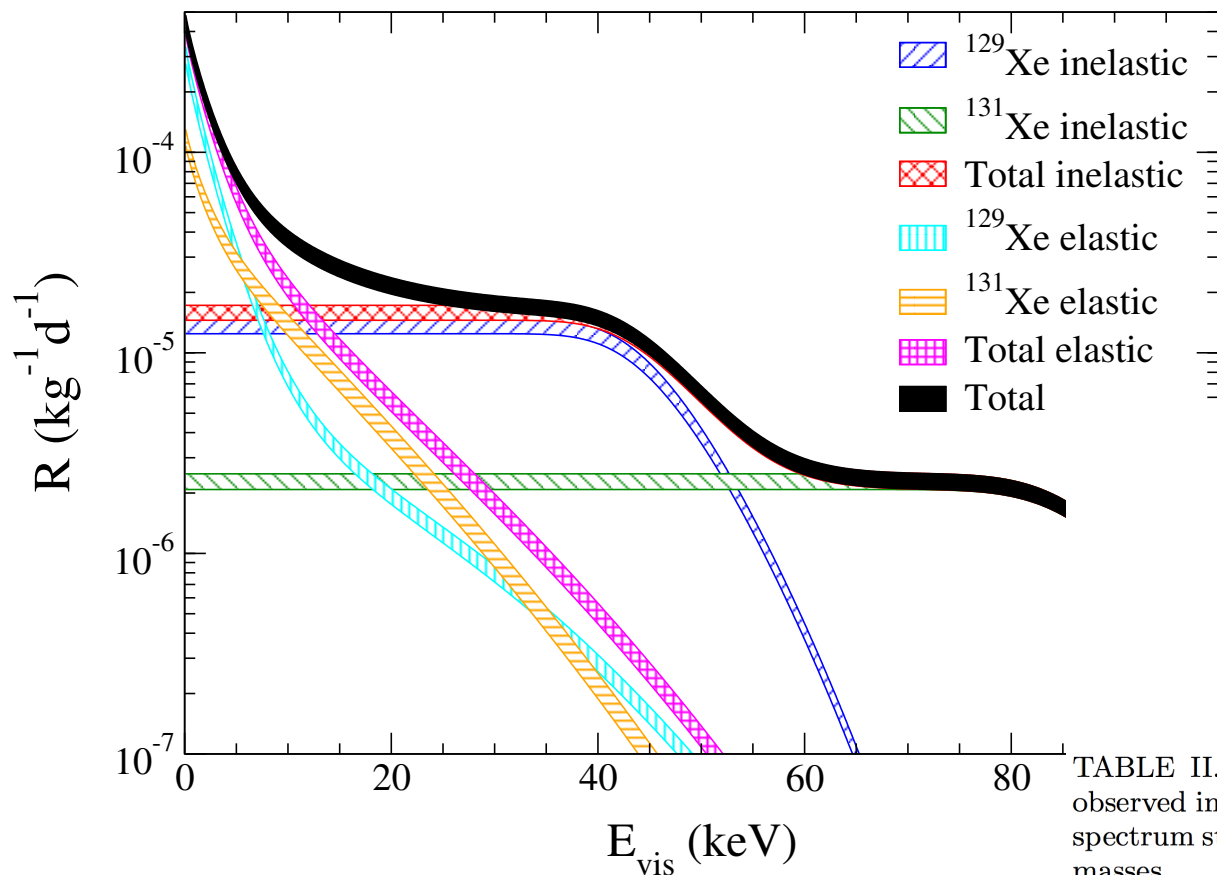


Signatures for **inelastic** WIMP scattering

elastic recoil + **prompt γ from de-excitation**

combined information from elastic and inelastic channel will allow to **determine dominant interaction channel** in one experiment

inelastic excitation sensitive to WIMP mass



Mass [GeV]	^{129}Xe	^{131}Xe	Total
10	—	—	—
25	5	—	5
50	7	17	9
100	7	24	12
250	9	32	19
500	11	35	24

TABLE II. Minimum energy E_{vis} in keV above which the observed inelastic spectrum for ^{129}Xe , ^{131}Xe and for the total spectrum starts to dominate the elastic one for various WIMP masses.

Chiral EFT for general WIMP-nucleon interactions

chiral symmetry implies a hierarchy for general responses with Q^v

Hoferichter, Klos, AS, PLB (2015)

WIMP	Nucleon	V		A	
		t	\mathbf{x}	t	\mathbf{x}
V	1b	0	1 + 2	2	0 + 2
	2b	4	2 + 2	2	4 + 2
	2b NLO	–	–	5	3 + 2
A	1b	0 + 2	1	2 + 2	0
	2b	4 + 2	2	2 + 2	4
	2b NLO	–	–	5 + 2	3

WIMP	Nucleon	S	P
S	1b	2	1
	2b	3	5
	2b NLO	–	4
P	1b	2 + 2	1 + 2
	2b	3 + 2	5 + 2
	2b NLO	–	4 + 2

SD interactions are axial-vector (A) – A interactions, SI is scalar (S) – S

2-body currents as large as 1-body currents in V-A channel

Chiral EFT for general WIMP-nucleon interactions

chiral symmetry implies a hierarchy for general responses with Q^v

Hoferichter, Klos, AS, PLB (2015)

	Nucleon	V	A
WIMP	t	\mathbf{x}	t
	1b	0	1 + 2
V	2b	4	2 + 2
	2b NLO	–	–
	1b	0 + 2	1
A	2b	4 + 2	2
	2b NLO	–	–

	Nucleon	S	P
WIMP	t	\mathbf{x}	t
	1b	2	1
S	2b	3	5
	2b NLO	–	–
	1b	2 + 2	1 + 2
P	2b	3 + 2	5 + 2
	2b NLO	–	–

matching to non-relativistic EFT

Fitzpatrick et al., JCAP (2013)

without chiral physics

$$\begin{aligned}
 O_1 &= \mathbb{1}, & O_2 &= (\mathbf{v}^\perp)^2, & O_3 &= i\mathbf{S}_N \cdot (\mathbf{q} \times \mathbf{v}^\perp), \\
 O_4 &= \mathbf{S}_\chi \cdot \mathbf{S}_N, & O_5 &= i\mathbf{S}_\chi \cdot (\mathbf{q} \times \mathbf{v}^\perp), & O_6 &= \mathbf{S}_\chi \cdot \mathbf{q} \mathbf{S}_N \cdot \mathbf{q}, \\
 O_7 &= \mathbf{S}_N \cdot \mathbf{v}^\perp, & O_8 &= \mathbf{S}_\chi \cdot \mathbf{v}^\perp, & O_9 &= i\mathbf{S}_\chi \cdot (\mathbf{S}_N \times \mathbf{q}), \\
 O_{10} &= i\mathbf{S}_N \cdot \mathbf{q}, & O_{11} &= i\mathbf{S}_\chi \cdot \mathbf{q},
 \end{aligned}$$

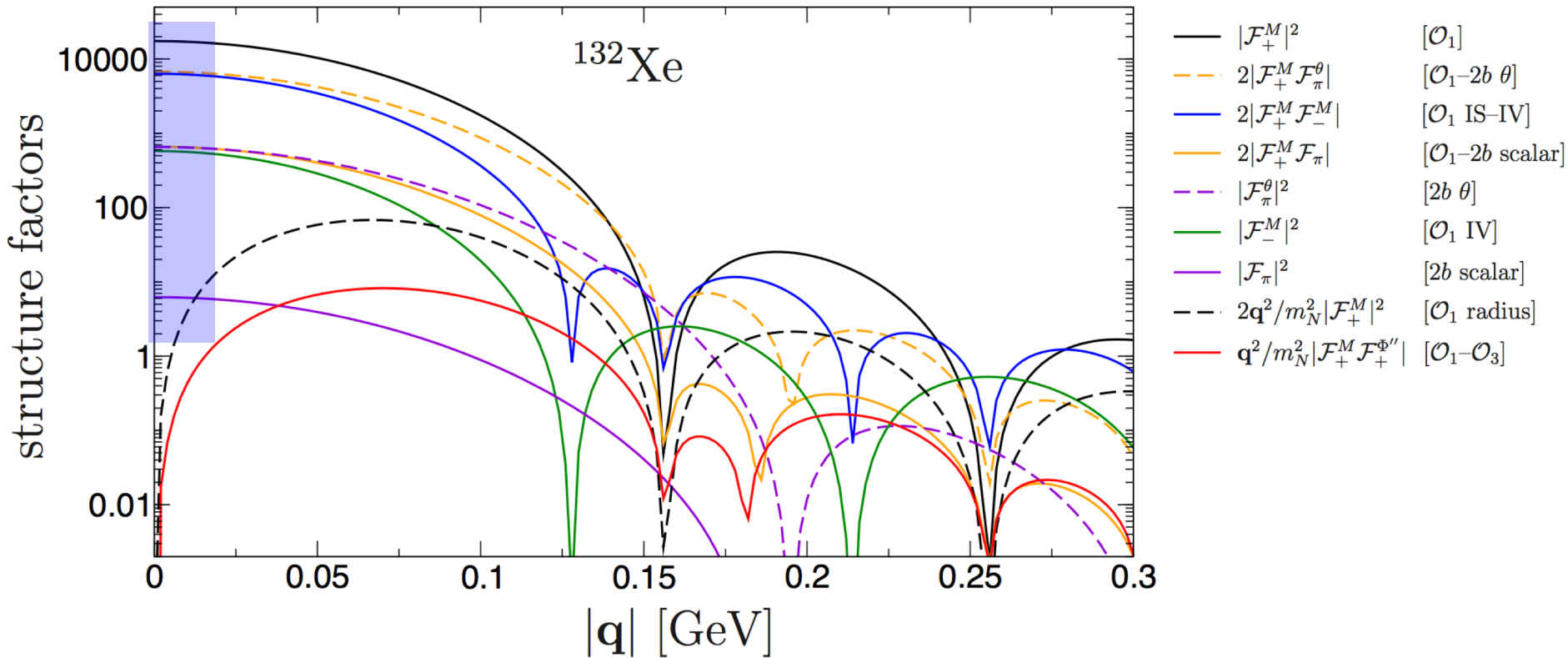
shows that NREFT operators are not linearly indep. (e.g., 4+6 are SD)

and not all are present up to $v=3$ (only 8 of 11 operators)

General coherent (SI+) WIMP nucleus scattering

for scalar currents: Hoferichter, Klos, Menéndez, AS, PRD (2016)

include all QCD effects + new operators that are coherent ($\sim A$)



dominant corrections are QCD effects: scalar current coupling to pion, isovector correction, radius correction to formfactor

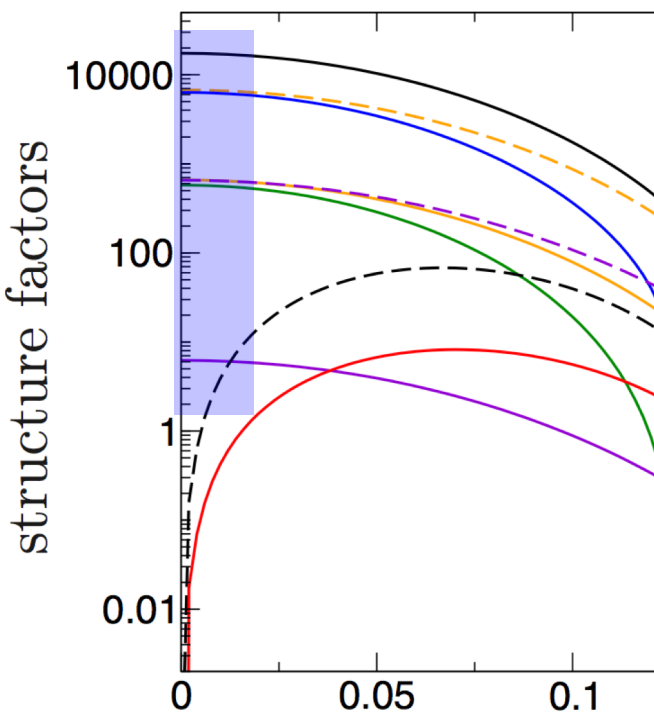
first new operator \mathcal{O}_3 contribution is 4 orders smaller

General coherent (SI+) WIMP nucleus scattering

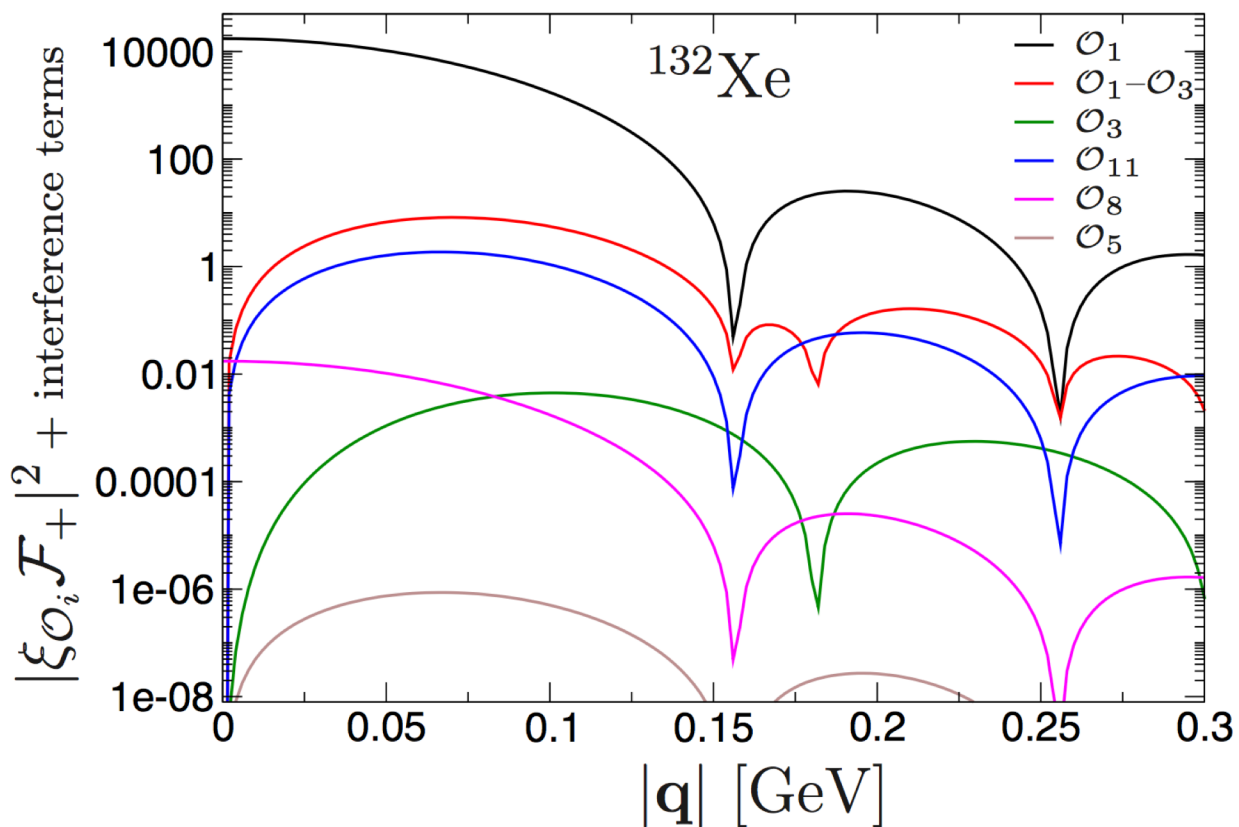
for scalar currents: Hoferichter, Klos, Menéndez, AS, PRD (2016)

include all QCD effects + new operators that are coherent ($\sim A$)

$$\begin{aligned}
 O_1 &= \mathbb{1}, & O_2 &= (\mathbf{v}^\perp)^2, & O_3 &= i\mathbf{S}_N \cdot (\mathbf{q} \times \mathbf{v}^\perp), \\
 O_4 &= \mathbf{S}_\chi \cdot \mathbf{S}_N, & O_5 &= i\mathbf{S}_\chi \cdot (\mathbf{q} \times \mathbf{v}^\perp), & O_6 &= \mathbf{S}_\chi \cdot \mathbf{q} \mathbf{S}_N \cdot \mathbf{q}, \\
 O_7 &= \mathbf{S}_N \cdot \mathbf{v}^\perp, & O_8 &= \mathbf{S}_\chi \cdot \mathbf{v}^\perp, & O_9 &= i\mathbf{S}_\chi \cdot (\mathbf{S}_N \times \mathbf{q}), \\
 O_{10} &= i\mathbf{S}_N \cdot \mathbf{q}, & O_{11} &= i\mathbf{S}_\chi \cdot \mathbf{q},
 \end{aligned}$$



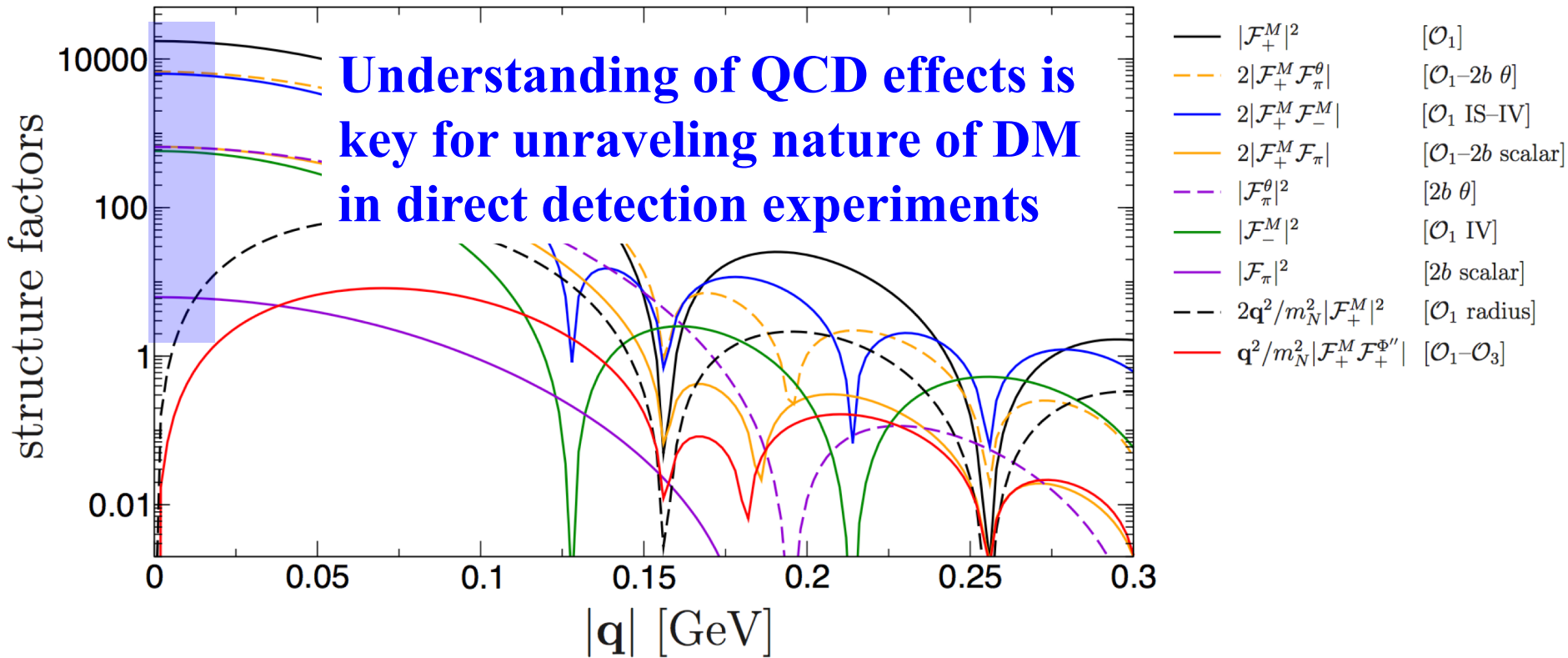
dominant corrections are
isovector correction, radi
first new operator O_3 cor



General coherent (SI+) WIMP nucleus scattering

for scalar currents: Hoferichter, Klos, Menéndez, AS, PRD (2016)

include all QCD effects + new operators that are coherent ($\sim A$)

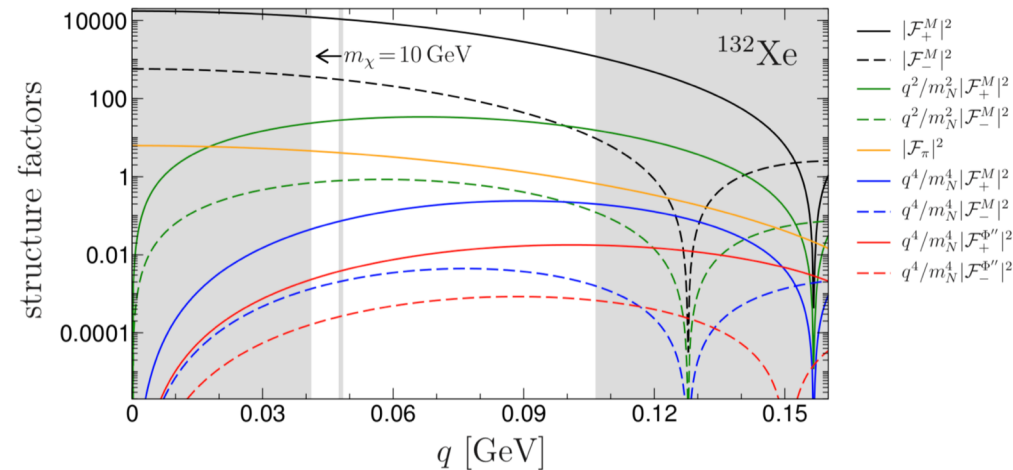


dominant corrections are QCD effects: scalar current coupling to pion, isovector correction, radius correction to formfactor

first new operator \mathcal{O}_3 contribution is 4 orders smaller

Disriminating different WIMP-nucleus response functions

Fieguth et al., PRD (2018) white region accessible to XENON-type experiment

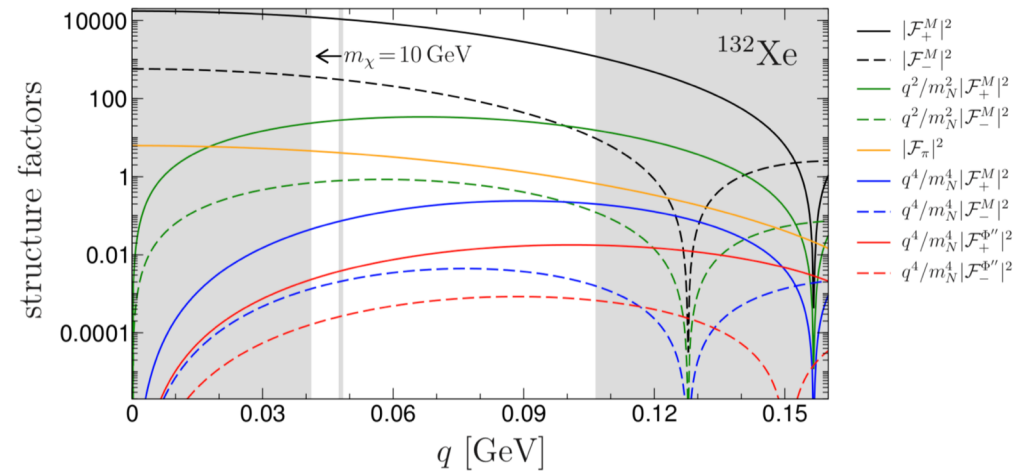


$$\frac{d\sigma}{dq^2} = \frac{1}{4\pi v^2} \left| \sum_{I=\pm} \left(c_I^M - \frac{q^2}{m_N^2} \dot{c}_I^M \right) \mathcal{F}_I^M(q^2) + c_\pi \mathcal{F}_\pi(q^2) + \frac{q^2}{2m_N^2} \sum_{I=\pm} c_I^{\Phi''} \mathcal{F}_I^{\Phi''}(q^2) \right|^2 + \frac{1}{4\pi v^2} \left| \sum_{I=\pm} \frac{q}{2m_\chi} \tilde{c}_I^M \mathcal{F}_I^M(q^2) \right|^2.$$

Can one discriminate responses in XENON1T, nT or DARWIN?

Disriminating different WIMP-nucleus response functions

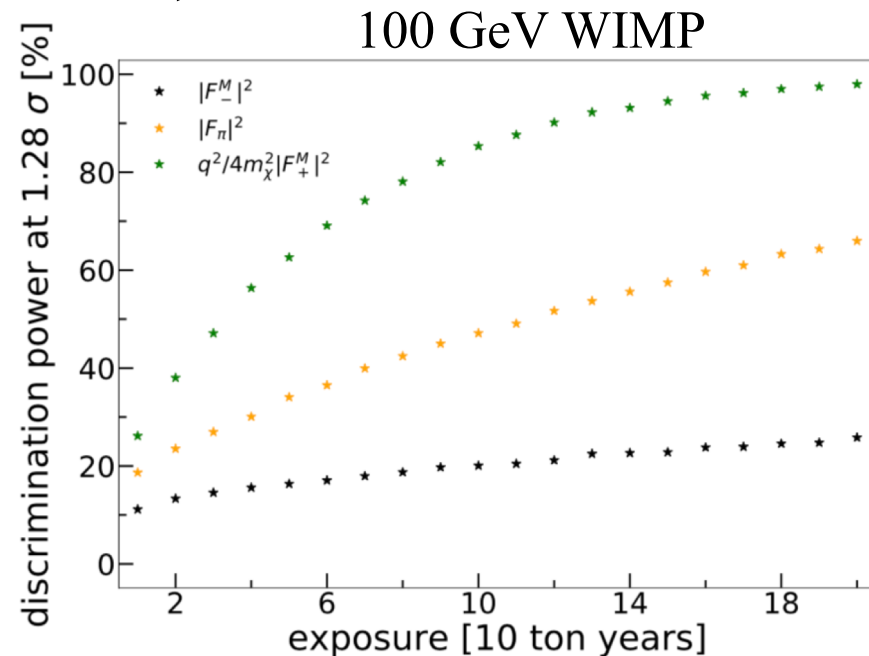
Fieguth et al., PRD (2018) white region accessible to XENON-type experiment



$$\frac{d\sigma}{dq^2} = \frac{1}{4\pi v^2} \left| \sum_{I=\pm} \left(c_I^M - \frac{q^2}{m_N^2} \dot{c}_I^M \right) \mathcal{F}_I^M(q^2) + c_\pi \mathcal{F}_\pi(q^2) + \frac{q^2}{2m_N^2} \sum_{I=\pm} c_I^{\Phi''} \mathcal{F}_I^{\Phi''}(q^2) \right|^2 + \frac{1}{4\pi v^2} \left| \sum_{I=\pm} \frac{q}{2m_\chi} \tilde{c}_I^M \mathcal{F}_I^M(q^2) \right|^2.$$

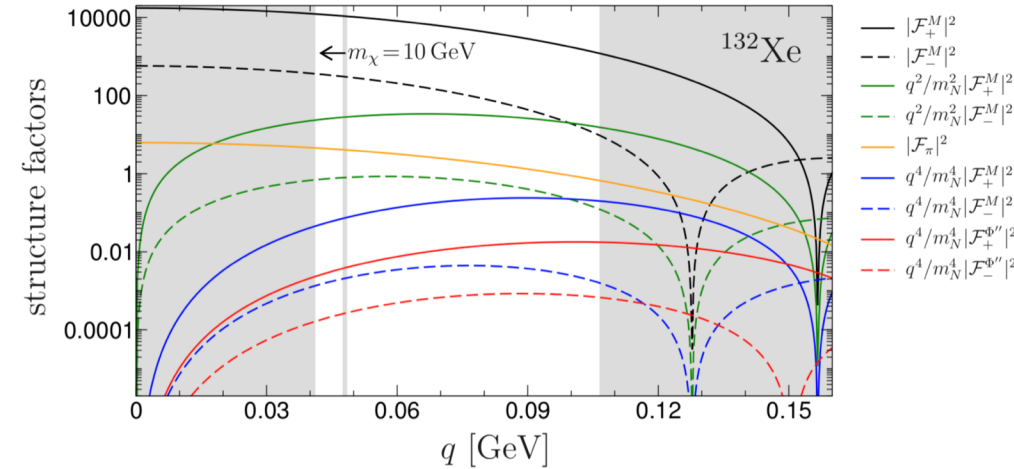
Can one discriminate responses in XENON1T, nT or **DARWIN**?
compared to standard SI response
(Helm form factor)

q-dependent responses more easily
distinguishable



Disriminating different WIMP-nucleus response functions

Fieguth et al., PRD (2018) white region accessible to XENON-type experiment



$$\frac{d\sigma}{dq^2} = \frac{1}{4\pi v^2} \left| \sum_{I=\pm} \left(c_I^M - \frac{q^2}{m_N^2} \dot{c}_I^M \right) \mathcal{F}_I^M(q^2) + c_\pi \mathcal{F}_\pi(q^2) + \frac{q^2}{2m_N^2} \sum_{I=\pm} c_I^{\Phi''} \mathcal{F}_I^{\Phi''}(q^2) \right|^2 + \frac{1}{4\pi v^2} \left| \sum_{I=\pm} \frac{q}{2m_\chi} \tilde{c}_I^M \mathcal{F}_I^M(q^2) \right|^2.$$

Can one discriminate responses in XENON1T, nT or **DARWIN**? compared to standard SI response (Helm form factor)

TABLE III: Discrimination power (in %) of a DARWIN-like experiment after 200 ton years of exposure.

m_χ	100 GeV			1 TeV		
	10^{-46}	10^{-47}	10^{-48}	10^{-45}	10^{-46}	10^{-47}
$ \mathcal{F}_-^M ^2$	94	26	12	100	35	13
$q^2/4m_\chi^2 \mathcal{F}_+^M ^2$	100	100	34	100	100	41
$q^2/4m_\chi^2 \mathcal{F}_-^M ^2$	100	98	25	100	100	32
$q^4/m_N^4 \mathcal{F}_+^M ^2$	100	100	55	100	100	63
$q^4/m_N^4 \mathcal{F}_-^M ^2$	100	100	47	100	100	53
$ \mathcal{F}_\pi ^2$	100	66	17	100	81	20
$q^4/4m_N^4 \mathcal{F}_+^{\Phi''} ^2$	100	100	58	100	100	69
$q^4/4m_N^4 \mathcal{F}_-^{\Phi''} ^2$	100	100	55	100	100	64

DARWIN could discriminate most responses, unless WIMP-nucleon cross section very small

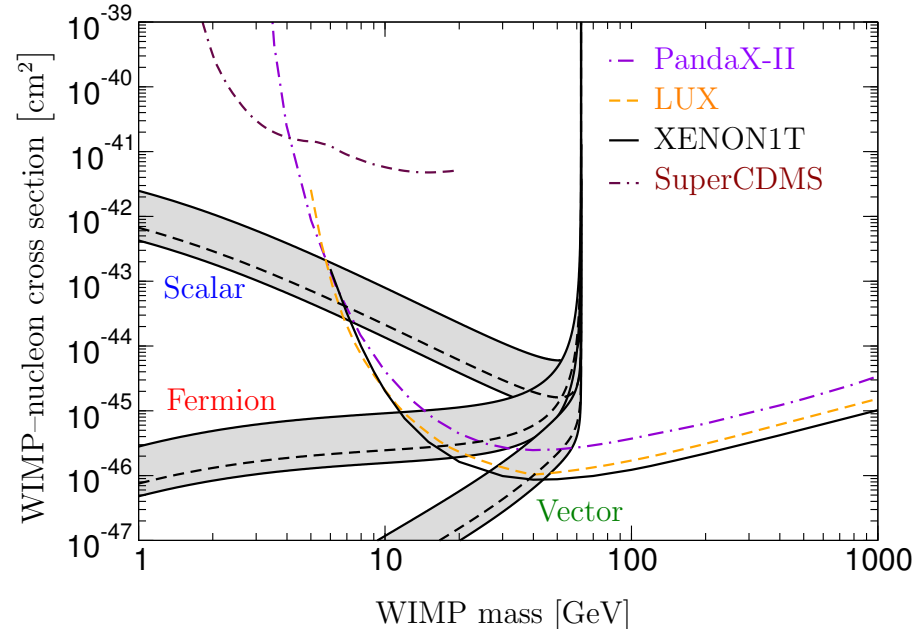
Higgs Portal dark matter

WIMP interacts with q, g via Higgs
fermion, **scalar** and **vector** WIMPS

for $m_h > 2m_\chi$ should be seen at LHC

linking LHC and direct detection
 requires Higgs-nucleon coupling

$$f_N = \sum_{q=u,d,s,c,b,t} f_q^N = \frac{2}{9} + \frac{7}{9} \sum_{q=u,d,s} f_q^N + \mathcal{O}(\alpha_s) \quad \text{use outdated input } f_N = 0.260 \dots 0.629$$



Higgs Portal dark matter

WIMP interacts with q, g via Higgs
fermion, scalar and vector WIMPS

for $m_h > 2m_\chi$ should be seen at LHC

linking LHC and direct detection
requires Higgs-nucleon coupling

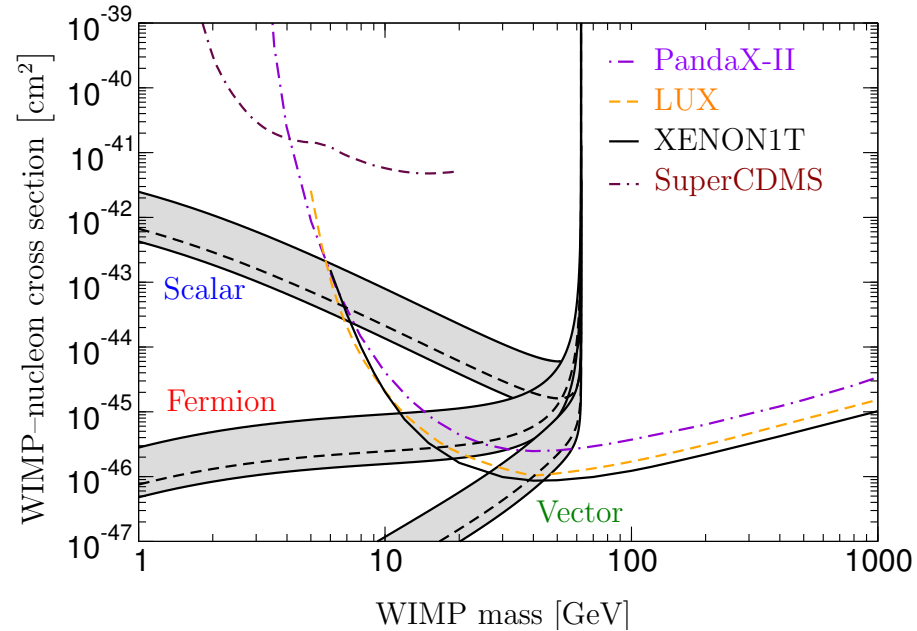
$$f_N = \sum_{q=u,d,s,c,b,t} f_q^N = \frac{2}{9} + \frac{7}{9} \sum_{q=u,d,s} f_q^N + \mathcal{O}(\alpha_s) \quad \text{use outdated input } f_N = 0.260 \dots 0.629$$

with new lattice results and χ PT: $f_N^{1b} = 0.307(9)_{ud}(15)_s(5)_{\text{pert}} = 0.307(18)$

two-body current contributions from scalar and trace anomaly coupling:
combine to coupling to pion and binding energy correction

$$f_N^{2b} = [-3.2(0.2)_A(2.1)_{\text{ChEFT}} + 5.0(0.4)_A] \times 10^{-3} = 1.8(2.1) \times 10^{-3}$$

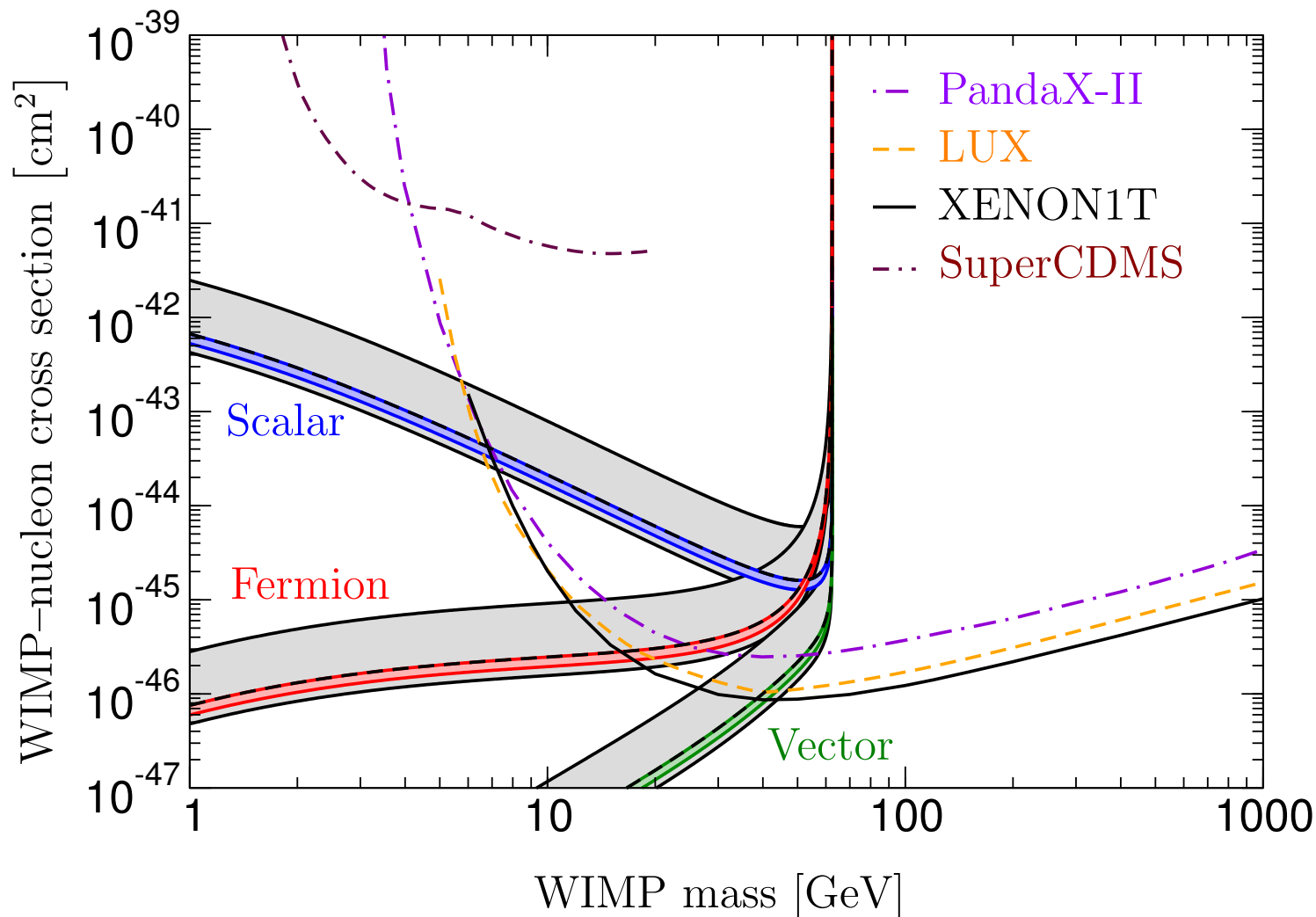
cancellation gives very small 2-body current contribution



Linking LHC and direct detection results in Higgs Portals

improved and consistent limits for Higgs Portals

Hoferichter, Klos, Menéndez, AS, PRL (2017)



Summary

Thanks to: **M. Hoferichter, P. Klos, J. Menéndez**

chiral effective field theory

nuclear forces and electroweak/WIMP/... interactions,
systematic for energies below ~ 300 MeV, so for direct detection

exciting era in nuclear physics of neutron-rich nuclei

with chiral EFT and powerful many-body calculations

structure factors for elastic/inelastic WIMP scattering

based on **large-scale nuclear structure calculations** and
systematic expansion of **WIMP-nucleon currents in chiral EFT**

incorporate what we know about QCD/nuclear physics

to go from future DM signal to nature of WIMP-quark interactions

improved and consistent limits for Higgs Portal dark matter